Lawrence Berkeley National Laboratory
Recent Work

Title
THREE EXPERIMENTS WITH HIGH ENERGY X-RAYS

Permalink
https://escholarship.org/uc/item/1813z463

Author
Rosengren, Jack W.

Publication Date
1952-08-01

eScholarship.org Powered by the California Digital Library
University of California

UNCLASSIFIED

UCRL-1913

c.2

UNIVERSITY OF CALIFORNIA — BERKELEY

TWO-WEEK LOAN COPY

This is a Library Circulating Copy which may be borrowed for two weeks. For a personal retention copy, call Tech. Info. Division, Ext. 5545

RADIATION LABORATORY

UCRL-1913
c.2

DISCLAIMER

This document was prepared as an account of work sponsored by the United States Government. While this document is believed to contain correct information, neither the United States Government nor any agency thereof, nor the Regents of the University of California, nor any of their employees, makes any warranty, express or implied, or assumes any legal responsibility for the accuracy, completeness, or usefulness of any information, apparatus, product, or process disclosed, or represents that its use would not infringe privately owned rights. Reference herein to any specific commercial product, process, or service by its trade name, trademark, manufacturer, or otherwise, does not necessarily constitute or imply its endorsement, recommendation, or favoring by the United States Government or any agency thereof, or the Regents of the University of California. The views and opinions of authors expressed herein do not necessarily state or reflect those of the United States Government or any agency thereof or the Regents of the University of California.

UCRL-1913

UNIVERSITY OF CALIFORNIA

Radiation Laboratory

Contract No. 7405-eng-48

THREE EXPERIMENTS WITH HIGH ENERGY X-RAYS

I. Angular Distribution of Photons in Showers

II. Angular Distribution of Bremsstrahlung Radiation

III. High Energy Photoprotons

Jack W. Rosengren
(Thesis)

August, 1952

Berkeley, California

Table of Contents

Table of Contents (contd.)

THREE EXPERIMENTS WITH HIGH ENERGY X-RAYS

I. Angular Distribution of Photons in Showers

II. Angular Distribution of Bremsstrahlung Radiation

III. High Energy Photoprotons

Jack W. Rosengren
(Thesis)

General Introduction

Near the end of the year 1948 under the supervision of its inventor, Professor E. M. McMillan, the construction of the Berkeley synchrotron was completed. The successful operation of this machine, the first in its energy range, made available in the laboratory x-rays with energies above 300 Mev in energy. It introduced the possibility of many new types of investigations and the extension of other studies to much higher energies.

This is a report of three experiments that were conducted utilizing the 322 Mev bremsstrahlung beam of this machine. Aside from being studies all employing high energy x-rays they are essentially unrelated. They have been presented in three independent parts, each with its own abstract and introduction.

I. ANGULAR DISTRIBUTION OF PHOTONS IN SHOWERS

Abstract

A study has been made of the angular distribution of the photons in electron-photon cascade showers initiated in Cu and Pb by high energy bremsstrahlung radiation. Targets of thicknesses 1.17, 2.52 and 5.30 radiation lengths of Pb and 0.85 radiation lengths of Cu were exposed individually to the 322 Mev bremsstrahlung beam of the Berkeley synchrotron. The angular distribution of all but the lowest energy photons emerging from the far side of the targets should be identical with the distributions at the same depths in an infinite medium.

The photons were detected by the beta-activity produced in Cu foils by the Cu^{63} (γ,n) Cu^{62} reaction. This reaction is known to be produced mainly by photons of energies near 17.5 Mev. Evidence is presented that the observed activity was not produced by electrons or neutrons.

The target thicknesses of Pb employed corresponded to depths in the shower of T/2, T, and 2T, where T is the depth of the shower maximum. Angular distributions were measured in the range from 6° to 50°. Rough agreement is shown between the results and the theoretical calculations of Eyges and Fernbach.

Introduction

For a theoretical interpretation of many experiments concerned with cascade photon-electron showers, application of so-called one dimensional shower theory is sufficient[e.g.1.]. This theory considers the longitudinal development of a shower under the assumption that there is no traverse spreading. For an interpretation of many experiments, particularly some concerning showers produced in air by cosmic rays, one needs to deal spedifically with this lateral development. Considerable theoretical work has been done on this subject. In general, one wished to find four distribution functions defined by the following:

$P_r(r,t,E)rdr$; the relative number of electrons of energy E at longitudinal depth t in the annular ring between r and r + dr independent of direction of motion.

$P_\theta(\theta,t,E)\theta d\theta$; the relative number of electrons of energy E at longitudinal depth t with velocity vectors in the solid angle between θ and $\theta + d\theta$ independent of lateral displacement from the shower axis.

$Q_r(r,t,E)rdr$ and

$Q_\theta(\theta,t,E)\theta d\theta$; the corresponding functions for photons.

Often, rather than seeking the distribution functions, the attempt is made to calculate the root mean square angular or radial displacement.

The first treatment of the lateral development of showers was given by Euler and Wergeland[2]; however, their results are now considered to give far too small an extension of showers. L. Landau[3] set up diffusion equations for the sidewise development, but his numerical results were in error. G. Moliere[4] has made an extensive investigation using an extension of Landau's method and has calculated the radial distributions of both electrons and

photons and the angular distribution of electrons. His work is carried out under approximation A*.

Roberg and Nordheim[6] have evaluated the mean square angular and lateral spreads of both electrons and photons at the shower maximum as functions of their energy.

Eyges and Fernbach have calculated the first several moments of the distribution functions and by means of a trial and error fitting have inferred the distributions. Using approximation A, they have determined the angular distributions of photons and electrons[7] and the radial distribution of electrons[8] at the depth of the shower maximum, t_{max}, and at 1/2 t_{max} and 2 t_{max}. They have also calculated all four distributions at the shower maximum, taking ionization losses into account, for E equal to twice the critical energy, ϵ, and for 5ϵ and 10ϵ[9,10].

In the past, most of the experiments involving photon-electron cascades dealt with the showers produced in the atmosphere by cosmic rays. Now with the availability of sufficiently high energy x-ray machines, experiments involving cascade showers can be done in the laboratory[e.g. 11,12].

Crowe and Hayward[13], using a cloud chamber in the 322 Mev bremsstrahlung beam of the Berkeley synchrotron, measured the energy spectrum and angular distribution of <u>electrons</u> at about the shower maximum in lead, obtaining reasonable agreement with theory. The purpose of the present experiment was to study the angular distribution of the <u>photons</u> in showers in lead.

<u>Qualitative Description of the Spread of a Shower</u>

The mechanism of the cascade shower is well known, the electrons pro-

---

*Rossi and Greisen[5], in their review article, introduce the notation "approximation A" for a treatment in which the ionization loss of electrons is neglected.

ducing numerous photons by radiation, the photons in turn forming electrons* by pair production. At high energies, Compton scattering and loss of energy by ionization are relatively unimportant. Since at these high energies the radiation and pair production processes propagate at very small angles with the forward direction, the shower develops essentially along a straight line, the number of particles multiplying, the average particle energy constantly decreasing. For the lower energy particles, ionization loss becomes important, and eventually the critical energy** is reached at which the average space rate of loss of energy by ionization is equal to that for loss by radiation. These lower energy particles are then lost to the shower as far as continued multiplication is concerned.

At a certain depth, t_{max}, in the shower medium, the attenuation processes start to exceed the cascade processes and the shower reaches a maximum development in number of particles, ionization, etc. Beyond this depth the shower declines; eventually it dies completely, and the energy of the incident primary electron or photon is reduced to heat energy of the gross medium.

Although until near its very end the main body of the shower proceeds directly forward, there is some lateral spreading from near the start. This spreading is caused almost completely by the multiple Coulomb scattering of the shower electrons by the nuclei of the medium. This process gives in one radiation length about ten times the deflection inherent in the radiation on pair production processes. The root mean square deviation, θ^2, acquired

---

*Throughout this paper, the term "electron" includes both positive and negative electrons.

**Definitions of the various terms used in shower theory are given in the review article by Rossi and Greisen[5].

The critical energy is the energy lost by an electron through ionization in one radiation length.

E critical is very roughly 600/Z Mev.

by an electron of energy E in one radiation length is roughly $\frac{E_s}{E}$, where E_s is the so-called characteristic energy*, about 21 Mev. The consequence of this energy dependence is that scattering becomes important only at lower energies and that, on the average a photon's deviation is due to the scattering of its most recent electron ancestors in the last few radiation lengths.

The high energy particles travel forward, maintaining a densely populated, very narrow central core (narrow when measured in radiation lengths).** Lower energy particles when formed are scattered outward from this core, diverging at large angles to give the shower its transverse spread. This expansion radially is not of indefinite extent; low energy particles do not cascade much and their energy is soon attenuated. The shower will spread to a limit determined by the range of the low energy particles, and this limit will be roughly maintained for the remainder of the shower's length, the low energy divergent particles being constantly supplied from the narrow, high energy, central core.

For photons and electrons of the same energy, the root mean square angular deviation of photons will be less than that of the electrons, since the deviation of photon is inherited directly from a higher energy electron. Because photons have longer mean free paths than electrons of the same energy, it happens that, despite the smaller angular deviation, the root mean square radial spread of the photons is larger than that of the electrons of the same energy.

---

* E_s, the "characteristic energy", is merely a constant with the dimension of an energy. $E_s = m_e (4\pi \cdot 137)^2 = 21$ Mev.

** A radiation length, the thickness Xo, is defined in gm/cm^2 by the equation $1/Xo = 4\pi n Z^2 r_o^2 \ln (183 Z^{-1/3})$. Where π = fine structure constant = 1/137 r_o = classical electron radius = 2.8×10^{-13} cm. Z = atomic number and n = number of atoms/gm. The radiation length is the fundamental unit of length of cascade shower theory. The description of radiation phenomena is only slightly dependent on Z when thicknesses are measured in terms of this unit.

Experimental Arrangement and Procedure for Measurement of Angular Distribution.

Arrangement

To determine the angular distribution of photons at various depths in a shower medium, the experimental arrangement shown in Fig. 1 was used. The 322 Mev bremsstrahlung beam of the Berkeley synchrotron, collimated to a diameter of one-quarter inch, impinged on a thick lead or copper target placed directly on the collimator wall. Photon-electron cascade showers were produced in the target medium, and these photons and electrons emerged from the far side traveling at various angles with the shower axis, which was the axis of the incident bremsstrahlung beam. The angular distribution of high energy particles at a given depth in a shower medium will in no way be determined by the material beyond that depth; therefore the angular distribution of the particles emerging from a target of thickness t will correspond to the distribution in an infinite medium at depth t.

Detectors

To detect the photons, the radioactivity produced by a (γ,n) reaction in copper was used. The .016" thick copper detector foils were positioned beyond the target on a lucite mount as shown in Fig. 1. The foils were mounted as segments of cylinders with the beam as their axis. The basic foil was three inches square, but to obtain reasonable angular resolution at larger angles, the foils were cut into two 1-1/2 inch strips or into four 3/4 inch strips and mounted as shown. The radial separation between the foils was 2 cm. (An expression for the relative effective solid angle per foil is derived in Appendix I.)

To obtain data between 5.5° and 30°, the mount was positioned 24 cm from the target. In this position each foil subtended an angle of about 2 degrees. To obtain data at larger angles, the mount was moved into a

position 11 cm from the target. In this close position only the four outer foil radii were used. The angles were between 30° and 55° and each foil subtended an angle of about 6 degrees. To monitor the incident beam flux, a .016" copper foil (not shown in Fig. 1) was placed between the collimator and the target where it intercepted the total incident beam.

The reaction used to detect the photons was Cu^{63} (γ ,n) Cu^{62}. The resulting Cu^{62} is beta-active with a ten minute half-life. The excitation curve for this (γ ,n) reaction has been extensively investigated[14,15]. The curve has a resonance shape with a peak at 17.5 Mev and a full-width at half-maximum of about 5.5 Mev; therefore, the photons detected in this experiment were of energy near 17.5 Mev.

Other investigations[16] have shown that a negligible fraction of the observed activity would be produced by electrons. The cross section for the Cu^{63} (γ ,n) Cu^{62} reaction is of the order 400 times the cross section for electro-disintegration. For comparison of experiment with shower theory, which is most reliable at high energies, it would have been desirable to use a detector sensitive to photons of energy higher than 17.5 Mev. Unfortunately such detectors (e.g. C^{12}(γ ,n) C^{11} peaked at about 27 Mev) have much lower cross sections, and also for many materials, the radioactivity produced is inconvenient to separate from that of more predominant low energy reactions. When one is limited to photons of energy of the order of 17.5 Mev, the comparison of experiment with theory should be most easily made for a high Z target medium, such as lead. This is because high Z materials have a low critical energy* and the present theory of lateral spread is re-

---

* Defined in footnote on page 3.

liable only for energies much above the critical energy.

Procedure

The experimental procedure was the following: After about a twenty-minute bombardment, the various fractional foils at a given angle were taped together with cellophane tape to form a standard three-inch square foil. To measure their beta-activity these foils were then rolled into the form of cylinders and were slipped over Victoreen 1B85 aluminum walled Geiger tubes. The activity of these foils relative to that of the monitor foil was determined by counting them all simultaneously for about fifteen minutes. Under these conditions only the desired ten minute beta-activity was observed.

Evaluation of Neutron Contribution

There is a possibility that the Cu^{62} radioactivity used to detect photons was produced by the Cu^{63} (n,2n) Cu^{62} reaction instead of by the (γ,n) process. To estimate the contribution of the (n,2n) process, the relative yield of the Al^{27} (n,p) Mg^{27} reaction was investigated using the same geometry. For the neutron spectrum to which the foils would be exposed, the Al reaction should have the larger cross section and its yield should set an upper limit on the yield of the Cu reaction[17,18*]. The Mg^{27} activity is convenient since it has about the same half-life of ten minutes as Cu^{62}, and there is no other comparable half-life in this region

---

*Cohen[17] measured the average cross sections for two reactions using the neutron spectrum produced by bombarding Be with 15 Mev deuterons and found:

Al^{27} (n,p) Mg^{27}	= 25 mb
Cu^{63} (n,2n)Cu^{62}	= 19.6 mb

The neutron spectrum produced by the synchrotron x-rays will be more predominantly low energy than in the case of Cohen's measurements. The lower threshold of the Al reaction will thus make its relative yield even larger.

of the isotope chart to interfere. The important point, of course, is that the Mg^{27} cannot be produced from aluminum by x-rays. When bombarded in the same geometry as the copper detector foils, a small activity was observed to be produced in the aluminum which, within statistical variations, decayed with a ten minute half-life. From the yield of this activity, an upper limit to the relative yield of the $Cu^{63}(n,2n)Cu^{62}$ process was estimated and is plotted as curve 6 in Fig. 2. It can be seen that thatneutron contribution may be important at large angles.

Results

General

The angular distributions of 17.5 Mev photons were measured at depths of 1.17, 2.52, and 5.30 radiation lengths in lead (7.60, 16.4, and 34.4 gm/cm^2 respectively)* and for 0.85 radiation lengths (11.3 gm/cm^2) in copper. These four curves, all normalized to the same incident flux at zero depth, are plotted in Fig. 2.

Also shown, as curve 5 of Fig. 2, is the relative intensity with no target; its spread being produced by interaction of the beam with the walls of the one-quarter inch collimator. This incident deviated radiation is not as important as it might first seem. At any reasonable depth in the shower medium, most of the 17.5 Mev photons observed will be descended from incident photons of appreciably higher energies; these higher energy quanta would exhibit much less spread upon emerging from the collimator than do the photons of curve 5.

For comparison with theoretical results the distribution curves at the three depths in lead are plotted individually in Figs. 3,4 and 5. It should be noted that each point represents the average of two or more determinations.

---

* The value of 5.9 gm/cm^2 given by Rossi and Greisen[5] for the radiation length in Pb has been increased by ten percent to agree with results of recent experiment[19].

2.5 radiation lengths is roughly the depth in lead of the shower maximum for 322 Mev bremsstrahlung incident. It is the depth where the transition curve for the photons producing the reaction Cu^{63} (,n)Cu^{62} has its maximum[11] and is about the depth of maximum ionization[12]. The other two depths, 1.2R.L and 5.3R.L., are in the vicinity of half and twice the depth of the shower maximum.

Normalization to Unit Incident Flux

The total flux (in arbitrary units) of photons near 17.5 Mev between about 5.5° and 50° was obtained by numerical integration of $2\pi \int_{5.5^\circ}^{50^\circ} I(\theta) \sin\theta d\theta$. The net flux between 0° and 5.5° was obtained experimentally for each depth using a circular copper detector foil which intercepted the central flux out to 5.5°. The yield of this foil relative to the monitor foil was normalized to the same conditions as for the detector foils at larger angles. Because of its smaller size the central foil beta-activities were counted on the Geiger tubes with higher efficiency than were those of the three inch square foils, and a correction factor of 0.80 (uncertainty ± 0.05) was necessary for normalization.

Neglecting the small contribution outside 50°, the total flux at the shower maximum was normalized to 1.55, which is known to be the value at this depth for unit flux incident at depth zero[11].*

Normalized in this manner, values of the flux through the central 5.5° and from 5.5° to 50° are given in Table I.

---

* This value was checked using a 1/4" collimator. A three inch square foil was placed in the usual monitor position directly preceding the lead and one was placed directly on the far side where it would intercept all the emerging flux. The value obtained was 1.54 ± .02.

Table I

Depth (Radiation lengths)	1.17 (Pb)	2.52 (Pb)	5.30 (Pb)	0.85 (Pb)
0° to 5.5°	0.891±0.5%	0.696±0.5%	0.340±0.7%	0.863±0.5%
5.5° to 50°	0.54	0.85	0.73	
Total, neglecting θ 50°	1.43	1.55	1.07	
Total, from Strauch's curve	1.24	1.55	1.00	

The values given for the central flux each represent the results of two or more determinations. The uncertainties quoted for these values are standard deviations based on counting statistics only, but should be the total uncertainties for the relative values. The values of total flux given in the fourth row are taken from Strauch's transition curve in lead for the photons responsible for $Cu^{63}(\gamma,n)\,Cu^{62}$.

It might be of interest to express the distribution curves in terms of the number of quanta per Mev interval at 17.5 Mev, per steradian, per equivalent quantum* incident at zero shower depth.

For the incident bremsstrahlung spectrum it is known that at 17.5 Mev

$$\frac{dN(e)}{QdE} = 0.0846 \quad \frac{\text{quanta}}{\text{Mev interval} \cdot \text{equivalent quantum}}$$

Then, since the distributions plotted in Figs. 2,3,4, and 5 are all as accurately as possible normalized to unit incident flux, we have

---

* The number of incident equivalent quanta Q is given by

$$Q = \frac{U}{E_{max}}$$

where U is the total incident energy, E_{max} is the upper limit of the bremsstrahlung.

$$\frac{dN(17.5\ \text{Mev})}{Qd\ dF} = 0.0846\ I(\theta)\ \frac{\text{quanta}}{\text{steradian} \cdot \text{Mev interval} \cdot Q}$$

where I (θ) is the value of the ordinate in the figures.

Angular Distribution at Small Angles

The angular distribution of photons of a given energy is very steep near the shower axis, theoretically the distribution has a $1/\theta$ singularity at the axis. This steepness at small angles is illustrated by the curve in Fig. 6, obtained at the depth of the shower maximum in lead. To get the data at the small angles, a geometry different from that using the three inch foils had to be employed. Instead of the usual 1/4 inch collimator, one 1/8 inch in diameter was used. The detectors were 5/32 inch copper discs positioned at various angles on a mount 43 cm from the lead target. At this distance, the diameter of each disc subtended an angle of 0.27°. The monitor was a 5/32" disc centered on the beam axis, and the data is plotted taking the intensity averaged over this disc as unity. Data was taken at angles from 1.4° to 6.8° as shown. The larger angle data (previously shown in Fig. 4) was arbitrarily normalized to give a smooth continuation of the curve. The curve shown was drawn to fit the data and is not based on theory.

Theoretical Angular Distribution Curves

Detailed predictions of the angular distribution functions for photons in showers have been given by Fyges and Fernbach[7,9,10]. They have calculated the distributions under the following conditions and assumptions:

(a) The pair production cross section is a constant for the energies considered and is taken as the asymptotic value.

(b) The incident photons or electrons which produce the showers are of much larger energies than the photons observed.

(c) For treatment of depths other than that of the shower maximum,

t_{max}: The photons observed have energies so much greater than the critical energy that ionization losses may be ignored (Approximation A).

(d) The scattering angles are small.

(e) One can uniquely determine the distribution function by a trial and error fitting of a curve to the known moments of the distribution function.

Do these conditions apply to 17.5 Mev photons in a shower produced in lead by incident 322 Mev bremsstrahlung? Condition (a) does not hold well. Near 17.5 Mev the pair production cross section is only 0.4 of the asymptotic cross section. Condition (b) does not hold well for an incident bremsstrahlung spectrum, but not as badly as it might first seem. Because of the multiplication and attenuation processes, the primaries producing the photons deep in the shower medium on the average must have considerably larger energies than the photons observed. Condition (c) obviously does not hold since the critical energy in lead is of the order of 7 Mev; however, it holds much better for lead than for lower Z materials. Condition (d) is worse for high Z materials since the scattering probability varies as Z^2. Nevertheless for electrons of energies quite a bit larger than 17.5 Mev, the condition holds fairly well. Assumption (e) has been experimentally tested by Eyges and Fernbach and they are confident of the accuracy of their method. The fitting of a distribution to values of its moments does not, however, determine the distribution with accuracy near the origin.

The distribution calculated by Eyges and Fernbach[7] for 1/2 t_{max}, t_{max}, and 2 t_{max} are shown in comparison with the experimental data in Figs. 3,4, and 5 respectively. Their curves were calculated in terms of the general

argument $\frac{E}{E_s}\theta$ (where E_s is the so-called characteristic energy, ~21 Mev), and have been evaluated for E = 17.5 Mev. At 1/2 t_{max} and 2 t_{max}, the only available curves are calculated in Approximation A. At the shower maximum, t_{max}, Eyges and Fernbach[9,10] have calculated, for different photon energies, a series of curves which do take ionization loss into account. Their distribution at t_{max} for E = 2 (where = critical energy, ~ 7 Mev in lead), evaluated for E = 17.5 Mev, is shown as the dotted curve in Fig. 4.

Discussion of Results

The distributions given by Approximation A are observed to give a fair fit at 1/2 t_{max}, but to become very poor with increasing depth, being too flat. This is to be expected since the effect of ionization loss would be to increase the average energy at which the scattering of the electronsancestors of the 17.5 Mev photons occurs. For angles above about 40° the experimental distributions seem to become much flatter, an effect which might be due to neutron backgrounds or to inadequate subtraction of Geiger counting background. The curve for t_{max} which takes ionization loss into account gives a reasonable fit to experiment for intermediate angles.

In general, the agreement in shape of the experimental distributions and the theoretical curves is better than might be expected since the comparison is made under circumstances where the conditions, as listed above, for real confidence in the theory have not been fulfilled.

II. ANGULAR DISTRIBUTION OF BREMSSTRAHLUNG RADIATION

Abstract

A measurement has been made of the angular distribution of the 322 Mev bremsstrahlung radiation from the Berkeley synchrotron. The bremsstrahlung is produced by bombarding an internal 0.020" thick Pt target. The photons were detected by the beta-activity induced in small Cu discs by the Cu^{63} (γ,n) Cu^{62} reaction. This reaction would be produced mainly by that part of the bremsstrahlung spectrum of energy near 17.5 Mev.

The angular spreading (of order of $6mc^2/E$) is observed to be much greater than the spread (of order mc^2/E) intrinsic in the bremsstrahlung production process. The theory of Schiff attributes this greater spread to the multiple Coulomb scattering of the electrons in the target before radiation. The observed angular distributions is compared with some theoretically predicted distributions and found to be considerably narrower. Its full width at half maximum is 9.2 ± 0.6 milliradians. This fact indicates an over estimate of electron scattering at 322 Mev, although the narrower distribution might be attributable to the special conditions present in a synchrotron.

Introduction

In addition to the intrinsic interest that it offers, the angular distribution of the bremsstrahlung radiation from a synchrotron is of considerable practical concern. It enters into such matters as the selection of optimum collimation, the determination of the total output of the machine, and the calculation of the bremsstrahlung spectrum passing through a collimator. The angular spread (full width at half maximum in radians) intrinsic in the bremsstrahlung radiation process is of the order mc^2/E where E is the total electron energy and mc^2 is the rest energy. The radiation from thick targets such as those in synchrotrons has, however, a considerably broader angular distribution, the full angle at half maximum being of the order $6mc^2/E$ for the 322 Mev Berkeley synchrotron. This increased spread is believed to be caused chiefly by the multiple scattering of the electrons in the target before radiation.

Schiff[20] has given a theory for the angular distribution of thick target bremsstrahlung based on the multiple scattering of the electrons in the target. Lanzl and Hanson[21], in an attempt to fit their own experimental data, have calculated somewhat narrower distributions than Schiff's using a different evaluation of the electron scattering.

The angular distribution of bremsstrahlung has been measured by various experimenters at lower energies. In the cases where a specialized target (often a wire) was used, there could be no direct comparison with theory. Koch and Carter[22], using a uniformly thick 0.005 inch Pt target at 19.6 Mev, found an angular distribution which within statistics agreed with Schiff's function. The distributions measured by Lanzl and Hanson[21] using various targets at 16.9 Mev are narrower than those predicted by Schiff but are in good agreement with their own calculations. Baldwin

et al.[23] have studied the angular distributions produced by 70 Mev electrons in synchrotron targets of various thicknesses and Z, finding excellent agreement with Schiff's theory for low Z but narrower distributions for high Z.

The following is a report of a study made of the angular distribution of the bremsstrahlung from the 322 Mev Berkeley synchrotron.

Theory

Intrinsic Spread (Thin Target Distributions)

Sommerfeld[24] and Schiff[25] have derived expressions for the intrinsic spread, which should be applicable to very thin targets. These expressions are obtained by integrating the Bethe-Heitler differential bremsstrahlung cross section over the angles of the scattered electron.* Sommerfeld's derivation does not include screening of the nuclei by their electron clouds, whereas the following expression obtained by Schiff takes screening into account:

$$\sigma(k,x)\,dkdx = 4\,Z^2 r_0^2 \frac{dk}{k} x\,d\,x\,F(x,k,E_0) \qquad (1)$$

where $F(x,k,E_0)$ is the angular distribution function

$$F(x,k,E_0) = \frac{16x^2E}{(x^2+1)^4E_0} - \frac{(E_0+E)^2}{(x^2+1)^2E_0^2} + \frac{E_0^2+E^2}{(x^2+1)^2E_0^2} - \frac{4x^2E}{(x^2+1)^4E_0} \ln M(x,k) \qquad (2)$$

$$\frac{1}{M(x,k)} = \left(\frac{mc^2k}{2E_0E}\right)^2 + \left(\frac{Z^{1/3}}{c(x^2+1)}\right)^2$$

* These results when in turn integrated over the photon angles give the Bethe-Heitler bremsstrahlung spectrum.

where

$a = 1/137$ = fine structure constant

E_o = incident electron energy

E = scattered electron energy

$k = E_o - E$ = radiated photon energy

$x = E_o\theta/mc^2$, the reduced angle

θ = angle between incident electron and photon

$r_o = e^2/mc^2$ = classical electron radius

$C = 183/\sqrt{\varepsilon} = 111$

ε = base of natural logarithms

This becomes the same as Sommerfeld's result when in $M(x,k)$ Z is set to equal zero (no screening). Complete screening holds when $\left(\frac{a^{1/3}}{C(x^2-1)}\right)^2 >> \left(\frac{mc^2k}{2E_oE}\right)^2$ i.e., k/E_o small.

The shape of the angular distribution is given by the function $F(x,k,E_o)$, which is proportional to the photon intensity per unit solid angle. For complete screening it is seen to depend on k and E_o as a function of k/E_o only. Actually the shape, plotted in terms of the reduced angle $x = E_o\theta/mc^2$ is only slightly dependent on k and E_o. As a consequence the radiation spectrum is roughly independent of angle, although low energy quanta are slightly more peaked toward $\theta = 0$.

Thick Target Distributions

The angular distribution of bremsstrahlung from thick targets was first treated by Schiff[20] with the following considerations: For small angles the William's multiple scattering theory[26] predicts the following angular distribution of electrons as a function of depth, t, into a target (normalized so that the integral over all angles is unity):

$$P(\theta,t) = \frac{1}{2\pi\beta t} \exp\left(-\theta^2/2\beta t\right) \qquad (3)$$

where $\beta = \left(\frac{9.2Ze^2}{E_o}\right)^2 N$

N = number of atoms per unit volume

E_o = electron energy

This assumes that the attenuation is negligible. Since radiation is equally probable at all depths t the effective angular distribution of the radiating electrons is the integral of Eq. (3) over the total target thickness x.

$$P(\theta) = \frac{1}{2\pi\beta} \left[-\mathrm{Ei}\left(-\theta^2/2\beta x\right)\right. \qquad (4)$$

where Ei is the exponential integral function given by

$$-\mathrm{Ei}(-y) = \int_y^\infty \frac{e^{-z}}{z}\, dz, > 0 \text{ for } 0 < y < \infty ,$$

and is tabulated in Jahnke and Emde[27].

Since the intrinsic radiation spread is narrow, compared with the spread of the electrons , the photons will be radiated essentially in the direction of the electron's line of motion and P(θ) will also be the angular distribution of the radiation. This is not true at angles of the order mc^2/E about θ = 0 since at these angles the intrinsic radiation spread becomes important in determining the distribution. (It might be noted that P(θ) given in Eq. (4) diverges at θ = 0). For small angles Schiff, by numerical calculations, folded together P(θ) and an expression for the intrinsic spread which was approximately the same as that of Eq. (2). He obtained finally for the intensity of radiation at angle θ, relative to that at θ = 0

$$I(\theta) = \frac{-\mathrm{Ei}\left(-\theta^2/2\chi x\right)}{\ln \frac{2\chi x E^2}{m^2 c^4} - 0.5772} \qquad (5)$$

$I(\theta)$ as given in Eq. (5) does not contain any dependence on k, the photon energy, and Schiff states that his numerical calculations indicated $I(\theta)$ was essentially independent of k.

Essentially the following derivation of the thick target bremsstrahlung angular distribution, which does not involve numerical integration, has been given by Lawson[28] and by Lansl and Hanson[21].

The function $F(\theta,k,E_o)$, eq. (2), for the intrinsic spread of the radiation may for small angles very accurately be approximated by the sum of two gaussians.

$$F(\theta,k,E_o) \sim a_1 \exp -(E_o\theta/mc^2\theta_1)^2 + a_2 \exp -(E_o\theta/mc^2\theta_2)^2 \qquad (6)$$

The constants a_1, a_2, θ_1, and θ_2 actually are slightly dependent on k, E_o and Z.

The electron multiple scattering distribution at depth t (normalized such that the integral over all angles is unity) may, for the small angles that concern us, be expressed as a gaussian function.

$$P(\theta, E, t) = \frac{E_o^2}{\pi bt} \exp (-E_o^2\theta^2/bt) \qquad (7)$$

When $F(\theta, k, E_o)$ and $P(\theta,E,t)$ are folded* together, we obtain the contribution to the angular distribution from radiation at target depth t.

$$I(\theta,k,E_o,t) = \frac{a_1 m^2c^4\theta_1^2}{m^2c^4\theta_1^2+bt} \exp -E_o^2\theta^2/(bt + m^2c^4\theta_1^2) \qquad (8)$$
$$+ \frac{a_2^2 m^2c^4\theta_2^2}{m^2c^4\theta_2^2+bt} \exp -E_o^2\theta^2/(bt+m^2c^4\theta_2^2)$$

---

* The convolution of two two-dimensional gaussian functions (written exp $-\theta^2/2\theta_1^2$ * exp $-\theta^2/2\theta_2^2$ is $\frac{2\theta_1^2\theta_2^2}{\theta_1^2-\theta_2^2}$ exp $-\theta^2/2(\theta_1^2-\theta_2^2)$ when θ_1 and θ_2 are small.

Integrating over the total target thickness T we obtain the net radiation pattern, normalized to unity at $\theta = 0$*.

$$I(\theta,k,E_o) = \frac{a_1\theta_1^2\left[\ln\left(1-\frac{E_o^2\theta^2}{bT-m^2c^4\theta_1^2}\right)+\mathrm{Ei}\left(\frac{-E_o^2\theta^2}{m^2c^4\theta_1^2}\right)\right]+a_2\theta_2^2\left[-\mathrm{Ei}\left(\frac{-E_o^2\theta^2}{bT-m^2c^4\theta_2^2}\right)-\mathrm{Ei}\left(\frac{-E_o^2\theta^2}{m^2c^4\theta_2^2}\right)\right]}{a_1\theta_1^2\ln\left[1-bT/m^2c^4\theta_1^2\right]+a_2\theta_2^2\ln\left[1-bT/m^2c^4\theta_2^2\right]} \qquad (9)$$

The value one obtains for the constant b in the gaussian approximation of the electron scattering distribution differs among the various multiple scattering theories. The theory of Moliere[29] which predicts somewhat narrower spreads than do the theories of Williams[26] and others, especially for large Z, appears to give the best fit to experiment[30]. Moliere's theory gives a very involved expression for $P(\theta,E,t)$; however, for any specific case a value of b can be obtained graphically which makes (7) a very good approximation.

Experimental Conditions and Procedure

Arrangement

The angular distribution of the bremsstrahlung from the Berkeley synchrotron was measured under the following conditions. The so-called short beam was used, in which case the rf accelerating voltage is turned off sharply at peak field. (For the "long beam" the envelope of the rf voltage is more gradually brought to zero, producing a beam spread out much more in time.) Loss of energy by radiation causes the electron orbit to collapse, electrons striking the Pt target on the inner wall over a period of about 20 μ sec.

---

* $-E_1(-\theta)$ diverges at $\theta = 0$, but $I(\theta)$ can be determined from the asymptotic expression $-E_1(-y_1) + E_1(-y_2) = \ln(y_2/y_1)$

The electron energy upon reaching the target has been estimated by Powell et al.[30a] to be 322 ± 6 Mev. During the collapse of the short beam, it is estimated that the radius of the electron orbit is reduced 3.0×10^{-4} cm per turn.

The target employed was the 0.020 inch thick Pb target that was in use in the Berkeley synchrotron during the period 1948-1951 and is the same thickness as the one now in the machine. The target was in the shape of a uniformly thick flag about 5/16" x 1" x 0.020". Its thickness represented 1.15 gm/cm^2 or about 0.18 radiation lengths.

Detectors

The bremsstrahlung was detected by the activity produced in small, 0.035" thick Cu discs of 1/8 inch diameter by the $Cu^{63}(\gamma,n)Cu^{62}$ reaction; hence, the angular distribution measured was that for photons of energies around 17.5 Mev (cf. p. 10). To maintain the detector discs in accurately determined positions during bombardment they were mounted on an Al frame in 1/8" diameter depressions spaced 0.15 inch apart as shown in Fig. 8. Actually, to obtain more activity, two discs, one behind the other were mounted at each point.

Since Fig. 8 is not drawn perfectly to scale it might appear that the Pb wall (usually used to collimate the beam) that is shown could produce some interference with the beam. Actually the aperature through which the beam passed subtended an angle of 62 milliradians, which is outside the angular range in which measurements were made. Effects due to scattering at the edges of the aperature would be negligible.

Procedure

The mount was centered in the bremsstrahlung beam using the relative activities induced in the Cu discs at the four positions immediately adjacent to the center. The usual method of aligning the apparatus using a

transit was not sufficiently accurate. In fact, when by means of photographic film the mount had been accurately centered in the beam passing through a 1/8 inch collimator, it was found to be about 6×10^{-4} radians (about 12 percent of the half angle of the cone at half intensity) from the position of maximum intensity. Actually for no run was the mount perfectly centered in the beam, but the position of the center could easily be determined from the data.

The procedure was to expose two to four detectors at a time, a detector at center serving as a monitor for each exposure. After a 15 to 20 minute bombardment the activities of the various discs were counted simultaneously for 15 minutes, using Victoreen mica-end-window Geiger tubes. The counting efficiencies of the different Geiger counters were normalized and continually checked using two uranium standards. The efficiencies were observed to remain constant and differed among the tubes by less than 6 percent.

Over a period of three months three separate measurements of the distribution were made. The distances from detector mount to the synchrotron target in the three cases were 81 inches, 165 inches and 184 inches. In the first measurement, data was taken along two perpendicular diameters through the center of the radiation pattern. In the other two cases, except for data taken just around the center to fix that point, measurements were made only along the horizontal radius in the direction AB shown in Fig. 1.

Results

The results of the three series of measurements are shown in Fig. 9.

The directions labeled in Fig. 9 are perhaps confusing. The direction denoted "left" refers to the horizontal direction labeled AB in the

plan diagram of Fig. 8. For the electrons striking the 0.020" Pt target this is the direction towards the closer target edge. The angles subtended by the diameters of the detector discs are indicated in the legend and were 1.85, 0.91 and 0.92 milliradians for series 1,2, and 3, respectively. The uncertainties shown are standard deviations based on counting statistics only. Also shown in Fig. 9 are the theoretical distributions given by Schiff[20], Eq. (5), and Lanzl and Hanson[21], Eq. (9). To evaluate Eq. (9), the values of the constants a_1, a_2, θ_1, and θ_2, were determined by a graphical fit of the intrinsic spread $F(x,k,E_o)$, Eq. (2), to be an $a_1 = 0.73$, $a_2 = 0.27$, $\theta_1^2 = 0.340$ radian^2, and $\theta_2^2 = 2.37$ radian^2. The value of bT appropriate to the 0.020 inch Pt target was determined from Moliere's theory[10] to be $244 \cdot m^2C^4$ radian^2. These values give the curve B shown in the figure. The curve C was obtained using the value $bT = 140 \cdot m^2C^4$ radian^2, which implies a multiple scattering spread 21 percent smaller than predicted by Moliere's theory.

The following features of the experimental data may be noted: There is no definite assymmetry within the angles of observation; one might expect the spread to be smaller in the direction of scattering out the target's edge. There seems to be somewhat of a disagreement among the three measurements. This inconsistency might be attributable to unknown differences in the operating conditions of the synchrotron, i.e., differences in the manner in which the electrons were striking the target. The measured distribution is narrower than the theoretical predicted radiation patterns. A reasonable fit, curve C, is obtained only when we assume the electron scattering to be considerably less than predicted by theory. The measured pattern has a full angle at half-maximum of 9.2 ± 0.6 mil-

liradians, which is 14 percent narrower than the curve of Lanzl and Hanson, and 22 percent less than the width of Schiff's distribution.

Discussion of the Results

A number of reasons may be listed as to why, in general, it is difficult to compare the angular distribution of bremsstrahlung from a betatron or synchrotron target with a theoretically predicted distribution.

(1) The target may not be of uniform thickness. Actually the standard target in many machines is in the form of a wire.

(2) Oscillations of the accelerated electrons cause them to strike the target at a variety of angles, tending to spread out the radiation distribution.

(3) The electrons because of the small pitch of their spiral path into the target strike close to the outer edge of the target. In the subsequent scattering of the electrons in the target, the ones scattered to larger radii may be scattered out of the target through its edge. This should lead to an asymmetry in the angular distribution of radiation. If the target is not perfectly normal to the entering beam it is conceivable the beam could nick the edge of the target without passing through the full target thickness. This condition would also lead to an asymmetry in the angular distribution of the bremsstrahlung.

(4) With thin targets multiple traversals of the electrons through the target will influence the resulting bremsstrahlung.

(5) Electrons deflected by the target through scattering or ionization loss will strike the walls of the donut accelerating chamber or elsewhere, producing radiation from secondary sources.

Of these possible objections, only (2) and (3) seem to apply to this measurement, limited to the component of the bremsstrahlung around 17.5 Mev at small angles. The effect of the oscillations of the electrons would be to broaden the angular distribution; hence, it can not account for too narrow a distribution. The effect of the electrons striking the edge of the target should be to produce an asymmetry in the radiation pattern, though perhaps only at large angles. This effect may account for the discrepancy at large angles between series (3) and series (1); however, in series (1), where the pattern has been measured in four directions, there is no definite asymmetry within the angles covered.

The fact that the measured distribution is somewhat narrower than those predicted by theory does not seem to be easily explainable by the circumstance that the measurement was made under the special conditions found in a synchfotron. The above results suggest that even Moliere's recent theory overestimates the scattering of high energy (300 Mev) electrons in high Z materials.

III. HIGH ENERGY PHOTOPROTONS

Abstract

An investigation has been made of the characteristics of the ejection of protons from various elements by high energy x-rays. Various targets were exposed to the 322 Mev bremsstrahlung beam of the Berkeley synchrotron, and the high energy protons produced were detected by means of a counter telescope consisting of three liquid scintillators. Each scintillator was viewed by two or three RCA-1P21 photomultiplier tubes with their outputs connected in parallel. The protons were required to stop in the second counter and a form of pulse-height analysis in the first counter was used to differentiate protons from less heavily ionizing particles (eg. mesons) of the same range. The minimum energy of the protons that could be detected by the telescope was 65 Mev.

The angular distributions of protons of energy near 70 Mev from Li, C and Ta were observed to be essentially identical and to have a large forward asymmetry. Evidence from C indicated that this asymmetry increases with energy. Over a wide range in energy the yield of photoprotons was found to be directly proportional to atomic number. Data were also obtained on the energy spectrum of the protons ejected from C from 70 Mev to above 200 Mev. The absolute differential cross section for the production of 72 Mev protons at 90° from C was found to be 0.72 ± 0.25 μb/Q-Ster-Mev.

A discussion is given of possible mechanisms for the production of these high energy photoprotons.

Introduction

The mechanisms for photodisintegration processes in nuclei are at present not well established. The characteristics of the emission of low energy particles from materials under x-ray bombardment can only in part be accounted for by the process of evaporation from the excited nucleus. Even for low excitation energies, of the order of 20 Mev., (γ,p) to (,n) ratios have been found[31] which are orders of magnitude higher than predicted by an evaporation model. The energy distributions of the emitted protons have high energy tails[32] which are much larger than for the maxwellian-like distribution from evaporation. This higher energy component has been found to differ from the lower energy protons in that its angular distribution is anisotropic[32]. These facts have been interpreted[33] as evidence for a direct photoelectric effect in which the photon interacts directly with one of the protons, ejecting it from the nucleus without forming a "compound nucleus" state.

Experiments with high energy bremsstrahlung, of the order of 300 Mev., have revealed the production in unanticipated number of protons with energies ranging up to above 200 Mev.[34,35,36,37]

Levinthal and Silverman[34] using proportional counters studied the protons produced by bombarding different materials with 322 Mev bremsstrahlung. They investigated the energy spectra from C, Cu and Pb at 90° from about 9 Mev to 70 Mev obtaining a yield proportional to E^{-s} where $s = 1.7 \pm 0.1$ for C, 1.9 ± 0.1 for Cu and 2.2 ± 0.2 for Pb. Their investigation of the Z dependence at 90° for production of 40 Mev protons revealed a yield closely proportional to Z. A measurement of the angular distribution of 40 Mev photoprotons from Be, C, and Cu revealed

distributions that were similar and that had large forward asymmetries..

The purpose of the present experiment was to extend the measurements of Levinthal and Silverman to higher proton energies. Recently Keck[35] has reported on somewhat similar experimental work with high energy photoprotons produced by 300 Mev bremsstrahlung. In any phases where the work of Keck and the present experiment overlap there is provided a comparison between results obtained with fairly different detector systems.

Recently Kikuchi[37] using nuclear emulsions in connection with a study of star production by high energy x-rays has gathered some quantitative and considerable qualitative knowledge of the production of photoprotons. More will be said of this in a discussion of the results of the present experiment.

The magnitude and the characteristics of the differential cross sections for the production of high energy photoprotons can definitely not be accounted for by an evaporation model. Various possible mechanisms have been suggested and each may account for some part of the observed production. Some of these possible mechanisms are the following:

(1) Compton process between the photon and an individual proton inside the nucleus. (The observed cross section for this process with a free proton is too small to account for much of the observed photoproton production).

(2) The interaction of a photon with a nucleon to form a high energy proton and a meson. (The meson may be absorbed in the remainder of the nucleus to form a star).

(3) Production of high energy protons upon reabsorption of a meson in the nucleus in which it was formed.

(4) A direct photoeffect wherein a photon interacts directly with an

individual nucleon or substructure of the nucleus such as a quasi-deuteron.

For the direct photoeffect Levinthal and Silverman[34] made some calculations based on independent proton wave functions using an emperical momentum distribution. Levinger[38] has made some quite detailed calculations using a quasi-deuteron model, i.e. an interaction of the photon with two closely interacting nucleons in the nucleus. Levinger's calculations were based on the calculations of Schiff[39] on the photodisintegration of the deuteron.

Experimental Arrangement

In this experiment an investigation was made of the protons emitted from various targets when bombarded with the high energy x-ray beam of the Berkeley synchrotron. Protons above an energy of 70 Mev were detected using a counter telescope of three liquid scintillation counters. A drawing of the general experimental arrangement is given in Figure 10.

The bremsstrahlung radiation from the Berkeley synchrotron is produced when the internal electron beam orbit collapses into the 0.020" Pt target near the inner wall of the donut acceleration chamber. For this pulse the rf accelerating voltage is modulated such that the electrons spill into the target over a period of about 3000 sec. The repetition rate of these pulses is six per sec. Because during these 3000 sec. the magnetic field is changing (it varies approximately as a 30 cycle sine wave) the electrons will strike the target at various energies. If the nominal energy can be taken to be 322 Mev then the electron energies actually ranged from 298-324 Mev. The net bremsstrahlung spectrum can be found by combining the bremsstrahlung spectra corresponding to the various quantum limits (electron energies) weighted by the relative beam intensities at these electron energies. In Figure 11 is given the resulting

bremsstrahlung distribution, the relative energy per energy interval plotted vs. photon energy. Curve A is for 322 Mev electrons striking the target, curve B, calculated by W. S. Gilbert, is roughly that given by the spread-out beam pulse.

As is shown in Figure 10, at 55 inches from the Pt target the synchrotron beam passed through a collimating hole in a lead wall nine inches thick. This hole was 3/4" in diameter at its entrance and was tapered, being part of a cone whose apex was at the synchrotron target. Beyond this collimator was a lead shield six inches thick with a hole for the beam about one inch in diameter; this hole was also part of a cone with the target at its apex. These collimators and the x-ray target were aligned by means of a transit.

The counter telescope was installed in a lead house with three inch thick walls to shield it from the general background radiation around the synchrotron. A 1-1/2 inch diameter hole in the front wall of the house determined the effective solid angle subtended by the counter telescope. The lead house was mounted on a carriage which could be revolved about the center of the x-ray target. The lead house was 11.4 inches from the target center, its aperture subtending a plane angle of 6°. To monitor the beam two ionization chambers, shown in Figure 10, that were part of the standard synchrotron installation were employed. The pre-collimator ionization chamber had been calibrated absolutely by Blocker and Kenney[40] and was relied on primarily.

Proton Detection and Identification

Particles were identified as protons essentially from their dE/dx and residual range. The counter telescope employed consisted of three

scintillation counters in line as shown in Figure 12. A particle's range was specified by demanding that it pass through the first counter and stop in the second. The protons were then distinguished from other particles by requiring a certain minimum pulse height in the first counter. By this method a deuteron would be recorded as a proton, but at the high energies investigated (corresponding to deuteron energies 90 Mev) it is doubtful if the deuteron contribution is appreciable.

The counter telescope employed in this experiment was built by the author in collaboration with W. S. Gilbert and was first used in an investigation of the photodisintegration of the deuteron at high energies[41]. The counters (cf. Figure 12) were liquid scintillators of terphenyl dissolved in toluene. The first counter, in which the particles dE/dx was investigated, was three inches in diameter, 1.6 gm per cm^2 of toluene in thickness, and was viewed from the side by three RCA-1P21 photomultiplier tubes with outputs connected in parallel. Counter 2, which consisted of 0.67 gm per cm^2 of liquid, and counter 3, which was 1.1 gm per cm^2 thick, were both four inches in diameter and were each viewed by two RCA-1P21 photomultiplier tubes. 2.6 gm per cm^2 of copper absorber were permanently placed between counters 1 and 2 to improve the discrimination of the telescope.

A block diagram of the electronics employed is given in Figure 13. The pulses from each counter were fed to a pulse height discriminator and gate former. For pulses from counters 2 and 3 these functions were provided by UCRL Inverter Discriminators. For counter 1, in which a form of pulse height analysis was made, the known high stability of the UCRL Linear Amplifier and Variable Gate warranted their use. The recovery time of the Variable Gate is long, approximately one sec, but because of the

large pulse demanded from the first counter its counting rate was always much lower than the rates in 2 and 3.

All three counters were connected in a coincidence circuit and the first two counters were connected in a separate double coincidence circuit. A subtraction of the two coincidence rates give the rate of particles stopping in the second counter. The coincidence circuits employed were crystal diode Rossi circuits known as UCRL Eight Channel Mixers.

A measure of the number of accidental double coincidences was given by a delayed coincidence channel, as shown in Figure 13. This channel gave the number of random coincidences between signals from counter 2 and signals from counter 1 that had been delayed by two sec. The gate lengths, the recovery time, and the resolution time of the electronics were all about 0.4 sec.

In identifying particles as protons it was necessary to distinguish protons from mesons. For particles of different masses and identical residual ranges the ratio of the dE/dx's in traversing matter is approximately $(m_1/m_2)^{0.44}$. In the case of protons and mesons, this ratio equals 2.3. This means that a proton would give up 2.3 times as much energy in counter No. 1 as would a meson, and if the scintillators were perfectly proportional, the proton pulse would be 2.3 times as large as the meson pulse. This ratio, call it the merit ratio, is a limiting maximum since it holds only for identical residual ranges or, to put it another way, for a second counter of zero thickness. In practice, counter No. 2 was of finite thickness and the ratio of the smallest proton pulse to the largest meson pulse was calculated to be 1.8. For protons the band of energies accepted was 62-71 Mev, with the corresponding energies given

up in the first counter being 20-17 Mev, respectively. For mesons the band was 28-32 Mev, and the energy lost in the first counter was 9.3-8 Mev, respectively. To examine higher energy particles, a copper absorber was inserted between the target and the counter telescope.

To ascertain the conditions under which one would be counting protons with full efficiency, a run was made using the 90 Mev neutron beam of the Berkeley 184-inch synchro-cyclotron. This neutron beam is obtained by deuteron stripping and has a wide spread in energy (a total width at half maximum of about 30 Mev). This beam was used to bombard a paraffin target, and since the energy is below the threshold for meson production, the particles observed will be almost entirely protons with a small fraction of heavier particles. The curve giving counting rate per unit beam vs. photomultiplier high voltage is shown in Fig. 14. The arrow indicates a standard point on the curve. The operating conditions of the first counter at this point were made reproducible by determining the singles counting rate of this counter with a beta source in a standard geometry. To be able to count the betas a standard 20 db attenuator, present in the output of the first counter during proton detection, was removed.

In Fig. 15 is shown an integral bias curve of coincidence counting rate vs. discriminator bias of the first counter obtained at 60° from a carbon target in the 322 Mev x-ray beam of the synchrotron. The arrow indicates the calibration point obtained using the 90 Mev neutron beam. The dotted curve indicates an ideal integral bias curve when there are only protons and π mesons. The maximum proton pulse is arbitrarily taken

as shown and the other points are calculated from range energy relations. The absolute value taken for the meson yield is based on the experimental data of Peterson, Gilbert and White[42].

The observed curve from carbon is affected by electrons at the low bias end and perhaps by deuterons at the large bias points. An operating point was selected at a bias five volts lower than the calibration point from the cyclotron run. From comparison of the ideal curve and the observed curve, it is believed that only protons were counted at the operating point and that the protons were counted with full efficiency.

To insure that the proper bias setting was constantly maintained during a given series of measurements frequent checks were made of the counting rate in counter 1 given by a beta source in a standard geometry (20 db attenuation removed, as mentioned above). These checks were made about once every hour during a run.

Experimental Measurements

Angular Distributions

The angular distributions of protons of energy near 70 Mev from Li, C and Ta were measured in the range from 30° to 150°, the results being given in Figs. 16, 17, 18, and 19. All values are plotted taking $d\sigma/Qd\Omega\, dE = 1$ at 90°. The boxes at each point indicate the standard deviations based on counting statistics only and the plane angle subtended by the detector system. The actual energies of the protons detected were for Li, 74 ± 8.2 Mev; C, 72 ± 8.5 Mev and for Ta, 69 ± 3 Mev. The energy spreads are due to the energy interval of the second counter and due to the energy loss in the targets.

For measurements made with $\theta < 90^\circ$ the targets were along the line at $\theta = 135^\circ$; for $\theta > 90^\circ$ the targets were along the line $\theta = 45^\circ$. Because of the high electron yield at the forward angles, thinner targets were employed at these angles. Adjustments of the data were made to take into account the fact that protons emitted at different angles suffer different energy losses in the target and the fact that different target thicknesses were used. This adjustment was made by determining the mean proton energy for each situation and correcting for the dependence of yield on energy (taking the measured dependence in C to hold for all three materials) and for the dependence of the effective energy interval of the second counter upon energy. This correction was at its largest eight percent for C and five percent for Li and Ta.

The angular distribution of photoprotons from carbon was also measured at angles from 11° to 45° for energies of 77 ± 12 Mev, 127 ± 8 Mev, and 174 ± 6.5 Mev. The results are shown in Fig. 21. In order to reach the angle of 11° it was necessary to move the detectors to a radius of 44 inches from the target center. For comparison the measurements at 20°, 30° and 45° were also made at this radius. At this distance the detection system subtended an angle of 2°. This was the only measurement in which the standard geometry previously described was not used.

Z Dependence

The Z dependence of photoproton production was investigated at two energies, 72 ± 10 Mev and 142 ± 5.5 Mev. The measurements were all made at an angle of $45 \pm 3^\circ$. The results are plotted in Fig.22. The targets employed in this study were ones that had been constructed by G. Igo and R. Eisberg especially for measurements of this kind. The targets were all about 1.5 gm/cm^2 in mass thickness and were all laminated in such a manner

as to all present the same physical thickness and area. Adjustment of the data was made to take account of the fact that the mean energy of the protons from the different targets differed slightly due to differences in energy loss in the targets. At its largest this correction amounted to three percent. Correction was also made for attenuation of the x-ray beam in the targets. This was done using the pair production cross section at 320 Mev and the correction at its largest was 15 percent in the case of Pb.

Energy Spectrum

The distributions in energy of the photoprotons produced at 45° and 90° in carbon by 322 Mev bremsstrahlung were measured for energies above about 70 Mev. The observed spectra are given in Figs. 23 and 24. The mean energy of protons accepted by the detector system was varied by placing Cu absorbers between the target and the first counter. For the measurements at 90° the absorbers were placed outside the lead house as shown in Fig. 12 but for measurements at 45° the apparatus was modified to permit the absorbers to be placed inside the lead house close to the first counter, precluding any effect due to multiple Coulomb scattering of the protons in the absorber.

As the mean energy was increased the thickness of the target was also increased to help maintain a reasonable counting rate. None of these carbon targets were so thick that it was necessary to correct for attenuation of the x-ray beam. When absorber sufficient to stop 330 Mev protons was in place a small counting rate was still observed. These counts were presumably produced through the agency of neutrons which produced protons in the absorber or perhaps in the first counter itself. For purposes of correcting the data for this background the yield from this effect was taken to be proportional to target thickness and independent of absorber. The correction was only appreciable, about 30 percent,

at the high energy points where conditions were similar to those under which the background was measured.

The data was corrected for nuclear absorption of protons in the Cu absorber. A cross section equal to the geometrical area was used, giving a mean free path, L, in Cu of 112 gm/cm^2. The correction factor, exp (x/L), ranged up to 1.60 for the thickest absorbers used. For the geometry used for the measurements at 90° a correction for loss due to multiple scattering was made which ranged up to 30 percent.

Absolute Cross Section

The absolute cross section for photoproton production from carbon at 90° and 72 Mev was measured to be 0.72 microbarns/eff. quantum, steradian, Mev. The major uncertainty in this measurement is due to uncertainty in absolute beam intensity. The absolute calibration of the beam monitor ionization chamber was done by R. W. Kenney and W. Blocker[40], who estimated the uncertainty as 20 percent. A comparison of the above experimental value with values obtained by other experimenters is given in Table II.

Table II

Comparison of Differential Cross Sections for 70 Mev Photoprotons at 90°

Worker	Method	Synchrotron Energy Mev.	μb/eff.quant. ster. Mev.	Maximum Likely Error
Levinthal and Silverman[34]	Proportional Counter	310	0.15	factor of 2
D. Walker[36]	Nuclear Emulsions	200	0.95	± 55 percent
J. Keck[35]	Scintillation Counter	300	0.74	- 30 percent
J. Rosengren	Scintillation Counter	310	0.72	- 35 percent
J. Levinger[38]	Calculation	200	0.25	factor of 3
J. Levinger[38]	Calculation	300	0.29	factor of 3

Summary of Results

Angular Distributions

At 70 Mev the angular distributions from Li, C, and Ta, as compared in Fig. 19, are within the precision of the measurements found to be identical. In Fig. 20 the observed distribution from C at 70 Mev is compared with that observed at 40 Mev by Levinthal and Silverman[34], and with that observed by Keck[35] at 100 Mev. There is no definite difference in the distributions at 40 and 70 Mev. The 100 Mev distribution found by Keck is somewhat higher between 90° and 30°. Other data of Keck at 130 Mev and 175 Mev show increasing forward asymmetries. This is also indicated in the data obtained at small angles from C as shown in Fig. 21.

Z Dependence

Like the data obtained for 40 Mev protons at 90° by Levinthal and Silverman and for 130 Mev protons at 67.5° by Keck, the present data at 45° for 72 and 142 Mev protons (Fig. 22) show yields directly proportional to atomic number. The straight lines drawn through the data in Fig. 22 have slopes of 1.06. The yields from Li and Ta, though not shown, when measured relative to C under somewhat different circumstances also showed the same direct dependence upon Z.

Energy Spectra.

The energy spectra of photoprotons from C observed at 45° and 90° (Figs. 23 and 24) seem to be smooth continuations of the $E^{-1.7}$ spectrum found by Levinthal and Silverman below 70 Mev at 90°. In the region of 140 Mev there appear to be breaks in the spectra similar to the break at 130 Mev observed by Keck at 67.5°. The slope beyond the break is at neither 45° nor 90° as steep as observed by Keck at 67.5°.

Absolute Cross Section

The value of 0.72 microbarns / eff. quantum-sterad-Mev for photoproton production from carbon at 72 Mev is in good agreement with the value found by Keck, but is considerably larger than the result obtained by Levinthal and Silverman. When an integration is made over the observed angular distribution at 72 Mev, one finds the value for the total cross section for photo-proton from carbon to be 9.9 ± 3.5 microbarns / eff. quanta - Mev.

Discussion of Theory and Results

A great deal of information on the mechanism of high energy photoproton production is given by the study made by Kikuchi[37] using nuclear emulsions. Exposing emulsions directly to high energy bremsstrahlung radiation with two different upper energy limits, 150 Mev and 300 Mev, Kikuchi studied the yields of single protons and protons from stars and compared their values for the two energy limits. His data as far as angular distributions and energy spectra are concerned are, within fairly large statistical uncertainties, in agreement with data obtained with counters. His results, however, tell much about the origin of these high energy protons. Kikuchi reports that for the photoprotons between 20 Mev and 60 Mev about half came from stars produced by x-rays above 150 Mev, the remainder were ones observed as single prongs. Half of these single protons were produced below 150 Mev and half above. For protons above about 60 Mev most came from stars produced by x-rays of energies above 150 Mev.

The theory of Silverman and Levinthal involving a direct photo effect can at most then only account for part of the protons of energies from 10 to 70 Mev that they observed. Their calculations were based on a direct correlation between the x-ray and proton energies; protons of energy E

being ejected by photons of energy E + 25 Mev. Actually it appears that three-fourths of the protons which they observed were produced by x-rays of energies above 150 Mev.

Kikuchi has suggested that the chief mechanism for photodissociation at high energies (x-ray energies above 140 Mev) might be what he calls the free meson effect. In this process mesons produced in the interior of a nucleus are reabsorbed with a subsequent dissociation of the nucleus. The basis for this suggestion is twofold. (1) Photo-meson production from various nuclei has been observed[43] to be proportional to the surface area of a nucleus (i.e. proportional to $A^{2/3}$), indicating absorption of those produced in the interior. (2) The studies by Kikuchi and Miller[44] show that the cross section for the photo production of stars increases markedly above the threshold for meson production.

Kikuchi then conjectures that the majority of photoprotons with energies between 20 and 60 Mev are protons ejected from the nucleus by the process in which the meson is initially formed. The large forward asymmetry for photoprotons of 40 Mev observed by Levinthal and Silverman is not incompatible with that expected for nucleon recoil from a meson.

This mechanism cannot account for the protons above about 60 Mev that were observed in this experiment. For exposure to 300 Mev bremsstrahlung there is not sufficient energy for a nucleon to recoil from a meson with energy much above 60 Mev.

If, as Kikuchi suggests, stars are produced by meson reabsorption within the nucleus in which it was formed then the protons above 60 Mev might be produced in this reabsorption process. The measured angular distributions for free meson production[45] are more or less isotropic and

and the protons resulting from the reabsorption process would then be expected to be roughly isotropic. Such is not the fact. As the results of this experiment show (Figs. 16 to 21), these high energy protons have a large forward asymmetry. Another mechanism must be sought].

Levinger[38], as was mentioned in the introduction, attempted to account for the high energy protons in terms of a direct photodissociation. Because the protons observed have large energies at large angles to the x-ray beam they must have had high momentum inside the nucleus before the photointeraction. This high momentum will be present if the proton is acted on by strong forces due to being very near other nucleons, i.e. much closer than the average spacing inside the nucleus. Levinger assumed that if a nucleon is very close to another nucleon it is probably not very close to a third and used in his calculations a quasi-deuteron model. Levinger's computations were based in turn on the calculations of Schiff[39] for the photodissociation of the deuteron.

The results of Levinger's calculations, while perhaps accounting for some of the characteristics of high energy photoproton production, have serious deficiencies. The absolute cross sections predicted (cf. Table II) are apparently a factor of four too low and no account was taken for the fact that only a fraction of the high energy protons produced by the primary process will leave the nucleus with their initial energy. If Levinger's model can be believed to be a good one then the indication is that the theory of Schiff on which Levinger's work is based predicts too low a result.

Actually Schiff only considered his results to be valid up to energies near 140 Mev since his calculations take only nucleon electric dipole and quadrupole transitions into account and do not consider meson effects.

Levinger, having nothing else available; employed these results at energies considerably above 140 Mev. Recent experiments[41,46] have revealed cross sections for deuteron photodisintegration at high energies that are much larger than predicted by Schiff. The evidence is that the cross section actually reaches a minimum near the threshold for meson production (near 140 Mev) and then increases. While the true angular distribution at these high energies (above 140 Mev) is still not definitely determined, it seems indicated that instead of the approximately $\sin^2\theta$ distribution (center of mass) given by Schiff, an isotropic distribution may be correct.

The above shows that one cannot expect Levinger's calculations closely to fit the experimentally observed high energy photoproton yields. The absolute cross sections predicted (cf. Table II) appear considerably too low. The angular distribution calculated for 70 Mev protons which is compared with experiment in Fig. 20 is not a very good fit.

Keck has interpreted the sharp break in the energy spectrum he observed at 67.5° as evidence for the validity of a deuteron model. This interpretation is based on the fact that the observed break occurred at about half the maximum bremsstrahlung energy, which should be true for a proton recoiling from a single nucleon rather than, for example, from the remainder of an alpha particle. If this interpretation is correct, the point of the break in the spectrum should depend on angle as given by the conservation equations for deuteron dissociation. The fact that the observed distributions at 45° and 90° (Figs. 23 and 24) are quite similar casts doubt on Keck's interpretation.

The calculated curves of Levinger for energy spectra were available to the author only from Levinger's article and were in a form such that they could not be accurately plotted for comparison with the results in

Figs. 23 and 24. Because of the presently known invalidity of the energy dependence used by Levinger for deuteron photodisintegration, his calculated spectra cannot be taken seriously. It can be said that below 100 Mev where the variation seems to be as $E^{-1.7}$ Levinger's curves are much steeper; hence, his curves do not show the observed breaks.

At present there are no adequate theoretical calculations to account for the characteristics of photoproton production. Because of the invalidity of the basic dissociation formulae used by Levinger, his calculations need to be repeated with appropriate corrections. There are indications that an application of his deuteron model using accurate empirical data for the deuteron photodissociation (when it is available) would lead to results closer to experiment.

An isotropic distribution for high energy deuteron photodisintegration (for which there is evidence) when used in Levinger's theory would lead to proton angular distributions of closer fit than shown in Fig. 20. More apparent, it would lead to roughly identical distributions for neutrons and protons. This would be in accord with the recent evidence[47] for a forward asymmetry for high energy photoneutron production, Levinger's calculations predicted a neutron distribution more or less symmetric about 90^0.

R. R. Wilson[48] has pointed out how the free meson effect suggested by Kikuchi and the model of Levinger are actually compatible. The effects predicted by both will occur if a large fraction of the time a meson when produced in a nucleus is absorbed by its parent nucleon's nearest neighbor, i.e. the other nucleon in a quasi-deuteron. The meson creation and reabsorption will then appear as a deuteron photodissociation, the system retaining the momentum of the proton.

Acknowledgements

It is with pleasure the author acknowledges the continued guidance and encouragement provided by Professor A. C. Helmholz in all phases of this work. He is indebted to Mr. N. Lewis for his assistance in many of the measurements of Parts I and II, and to Mr. J. Dudley for his invaluable cooperation in the experiments of Part III. The counter system employed in the photoproton measurements was developed in cooperation with Dr. W. S. Gilbert, Thanks are due Mr. John Barale and others of the Electronic's Group for assistance with the electronics employed. Grateful appreciation is given Mr. George McFarland and the entire synchrotron crew for their cooperation in use of the machine.

Appendix

Solid Angle Calculation

The geometry of the detector foils used in the study of the aggular distribution of photons in showers is shown in Figs. 1 and 7.

Let l = length of foil along circumference (cf. Fig. 7)

Let n = number of atoms per unit area of foil

Let σ = cross section per atom

Referring to Fig. 7, the solid angle subtended by one atom in the interval dx is σ/r^2, and the total solid angle subtended by atoms in dx is

$$d\Omega = (\sigma/r^2)\, n\, l\, dx$$

In terms of the angle θ:

$$dx = r d\theta/\sin\theta$$

and

$$r = R/\sin\theta$$

Then

$$d\Omega = l\, n\, \sigma\, d\theta/R$$

To find the total solid angle subtended by the atoms in a foil we integrate over $d\theta$ and obtain finally:

$$\Omega = l\, n\, \sigma\, \phi/R$$

Then to find the relative photon intenstiy we weigh the relative activity of a given foil with the factor $R/l\,\phi$ since n and σ are identical for all foild.

References

1. L. Eyges, Phys. Rev. 81, 981 (1951)

2. H. Euler and H. Wergeland, Astrophys. Nor. 3, 165 (1940); Naturwiss. 28, 41 (1940)

3. L. Landau, J. Phys. U.S.S.R. 2, 234 (1940)

4. G. Moliere, Cosmic Radiation, W. Heisenberg ed. New York, Dover Publications, 1946, p 26 Phys. Rev. 77, 715 (1950)

5. B. Rossi and K. Greisen, Rev. Mod. Phys. 13, 240 (1941)

6. J. Roberg and L. W. Nordheim, Phys. Rev. 75, 444 (1949)

7. L. Eyges and S. Fernbach, Phys. Rev. 82, 287 (1951)

8. S. Fernbach, Phys. Rev. 82, 288 (1951)

9. L. Eyges and S. Fernbach, Angular and Radial Distributions of Particles in Cascade Showers, University of California Radiation Laboratory Report No. UCRL-943, October 5, 1950

10. L. Eyges and S. Fernbach, Phys. Rev. 82, 23 (1951)

11. K. Strauch, Phys. Rev. 81, 973 (1951)

12. W. Blocker, R. W. Kenney, and W.K.H. Panofsky, Phys. Rev. 79, 419 (1950)

13. K. Crowe and E. Hayward, Phys. Rev. 80, 40 (1950)

14. B. C. Diven and G. M. Almy, Phys. Rev. 80, 407 (1950)

15. H. E. Johns, L. Katz, R. A. Douglas, R. N. H. Haslam, Phys. Rev. 80, 1062 (1950)

16. L. S. Skaggs, J. S. Laughlin, and L. H. Lanzl, Phys. Rev. 73, 1223, (1948)

17. B. L. Cohen, Phys. Rev. 81, 184 (1951)

18. J. L. Fowler and J. M. Slye, Jr., Phys. Rev. 77, 787 (1950)

19. J. L. Lawson, Phys. Rev. 75, 433 (1949 and R. L. Walker, Phys. Rev. 76, 527 (1949)

20. L. I. Schiff, Phys. Rev. 70, 87 (1946)

21. L. H. Lanzl and A. O. Hanson, Phys. Rev. 83, 957 (1951)

References (contd)

22. H. W. Koch and R. E. Carter, Phys. Rev. 77, 165 (1950)

23. G. C. Baldwin, F. I. Boley, and H. C. Pollack, Phys. Rev. 79, 210 (1950)

24. A. Sommerfeld, Wellenmechanik (Ungar, New York), p. 551

25. L. I. Schiff, Phys. Rev. 83, 252 (1951)

26. E. J. Williams, Phys. Rev. 58, 292 (1940)

27. E. Jahnke and F. Emde, Tables of Functions, New York, Dover Publications 1943, p. 6

28. J. D. Lawson, Proc. Phys. Soc. A63, 653 (1950)

29. G. Moliere, Z. Naturforsch. 3a, 78 (1948)

30. A. O. Hanson, L. H. Lanzl, E. M. Lyman, and M. B. Scott, Phys. Rev. 84, 634 (1951)

30a. W. M. Powell, W. Hartsough, and M. Hill, Phys. Rev. 81, 213 (1951)

31. O. Hirzel and H. Waffler, Helv. Phys. Acta 20, 373 (1947)

32. B. C. Diven and G. M. Almy, Phys. Rev. 80, 407 (1950)

33. E. D. Courant, Phys. Rev. 82, 703 (1951)

34. C. Levinthal and A. Silverman, Phys. Rev. 82, 822 (1951)

35. J. C. Keck, Phys. Rev. 85, 410 (1952)

36. D. Walker, Phys. Rev. 81, 634 (1951) Phys. Rev. 84, 149 (1951)

37. S. Kikuchi, Phys. Rev. 86, 41 (1952)

38. J. S. Levinger, Phys. Rev. 84, 43 (1951)

39. L. I. Schiff, Phys. Rev. 78, 733 (1950)

Similar calculations have been made by J. F. Marshall and E. Guth, Phys. Rev. 76, 1880 (1949) Phys. Rev. 78, 739 (1950)

40. W. Blocker, R. W. Kenney and W. K. H. Panofsky, Phys. Rev. 79, 419 (1950) E. M. McMillan, W. Blocker and R. W. Kenney, Phys. Rev. 81, 445 (1951)

41. W. S. Gilbert and J. W. Rosengren, Deuteron Photodisintegration at High Energies, Univ. Calif. Radiation Laboratory Report No. UCRL-1792, May 9, 1952; Bull Am. Phys. Soc. 26, No. 8 (1951)

References (contd.)

42. J. M. Peterson, W. S. Gilbert and R. S. White, Phys. Rev. 81, 1003 (1951)

43. R. F. Mozley, Phys. Rev. 80, 493 (1950); R. M. Littauer and D. Walker, Phys. Rev. 82, 746 (1951)

44. R. D. Miller, Phys. Rev. 82, 260 (1951); S. Kikuchi, Phys. Rev. 81, 1060 (1951)

45. A. Bishop, J. Steinberger and L. Cook, Phys. Rev. 80, 291 (1950)

46. T. S. Benedict and W. M. Woodward, Phys. Rev. 85, 924 (1952); S. Kikuchi, Phys. Rev. 85, 1062 (1952); R. Littauer and J. Keck, Phys Rev. 86, 1051 (1952)

47. D. W. Kerst, L. J. Koester, A. S. Penfold, and J. H. Smith, Bull Am. Phys. Soc. 27, No. 3 (1952)

48. R. R. Wilson, Phys. Rev. 86, 125 (1952)

Figure Captions

1. Experimental arrangement for measurement of angular distribution of shower photons.
2. Angular distributions of 17.5 Mev. shower photons at various shower depths, 322 Mev bremsstrahlung incident.
3. Angular distribution of 17.5 Mev shower photons at 1.2 radiation lengths depth in lead (mislabeled 1.7 radiation lengths).
4. Angular distribution of 17.5 Mev shower photons at 2.5 radiation lengths depth in lead.
5. Angular distribution of 17.5 Mev shower photons at 5.3 radiation lengths depth in lead.
6. Angular distribution (including small angles) of 17.5 Mev shower photons at 2.5 radiation lengths depth in lead.
7. Geometry of detector foils for measuring angular distribution of shower photons.
8. Experimental arrangement for measurement of the angular distribution of bremsstrahlung radiation.
9. Angular distribution of 17.5 Mev photons in the 322 Mev bremsstrahlung beam of the Berkeley Synchrotron.
10. Plan diagram of the experimental arrangement for the study of photoprotons.
11. Bremsstrahlung distributions; energy per energy interval vs. x-ray energy.
12. Proton counter telescope.
13. Block diagram of electronics.
14. Voltage plateau for detection of protons produced by 90 Mev neutron beam.
15. Representative bias plateau for detection of photoprotons.

Figure Captions (contd.)

16. Angular distribution of 74 Mev photoprotons from lithium.
17. Angular distribution of 72 Mev photoprotons from carbon
18. Angular distribution of 69 Mev photoprotons from tantalum.
19. Angular distributions of photoprotons near 70 Mev from Li, C, and Ta.
20. Angular distributions of photoprotons from carbon.
21. Angular distributions of photoprotons from carbon, small angles.
22. Z dependence of photoproton production.
23. Energy spectrum of photoprotons from carbon at 45°.
24. Energy spectrum of photoprotons from carbon at 90°.

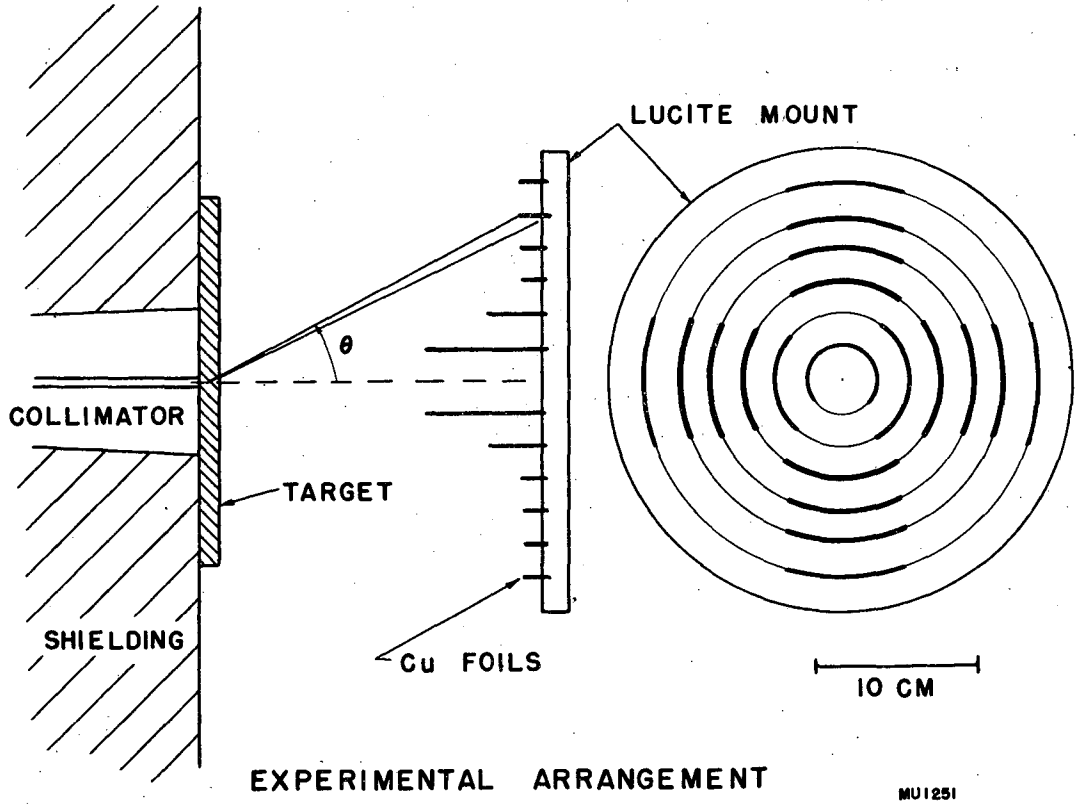
LUCITE MOUNT
θ
COLLIMATOR
TARGET
SHIELDING
Cu FOILS
10 CM
EXPERIMENTAL ARRANGEMENT
MU1251

Fig 1

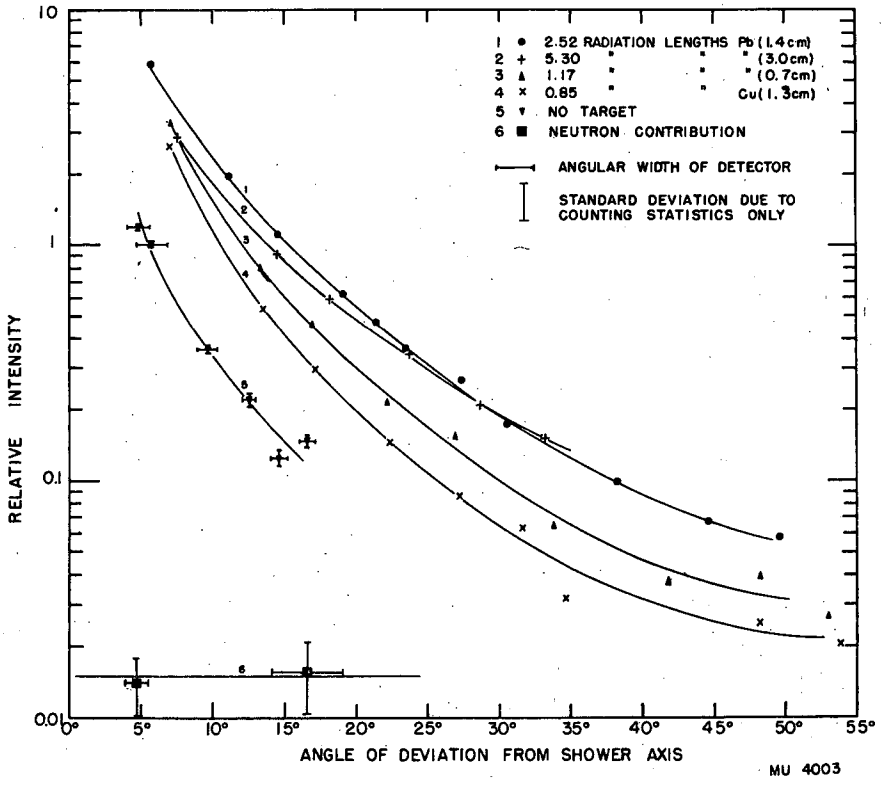
1 ● 2.52 RADIATION LENGTHS Pb (1.4 cm)
2 + 5.30 " " " (3.0 cm)
3 ▲ 1.17 " " " (0.7 cm)
4 × 0.85 " " Cu (1.3 cm)
5 ▼ NO TARGET
6 ■ NEUTRON CONTRIBUTION
ANGULAR WIDTH OF DETECTOR
STANDARD DEVIATION DUE TO COUNTING STATISTICS ONLY
RELATIVE INTENSITY
10
1
0.1
0.01
0°
5°
10°
15°
20°
25°
30°
35°
40°
45°
50°
55°
ANGLE OF DEVIATION FROM SHOWER AXIS
MU 4003

Fig. 2

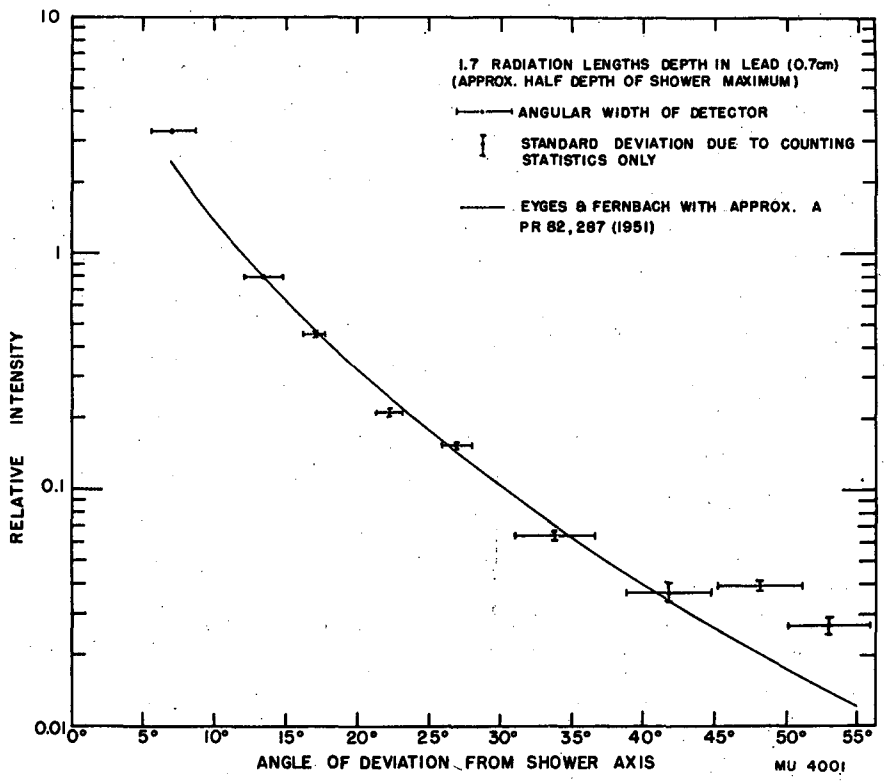
1.7 RADIATION LENGTHS DEPTH IN LEAD (0.7cm)
(APPROX. HALF DEPTH OF SHOWER MAXIMUM)
ANGULAR WIDTH OF DETECTOR
STANDARD DEVIATION DUE TO COUNTING STATISTICS ONLY
EYGES & FERNBACH WITH APPROX. A
PR 82, 287 (1951)
RELATIVE INTENSITY
10
1
0.1
0.01
0°
5°
10°
15°
20°
25°
30°
35°
40°
45°
50°
55°
ANGLE OF DEVIATION FROM SHOWER AXIS
MU 4001

Fig. 3

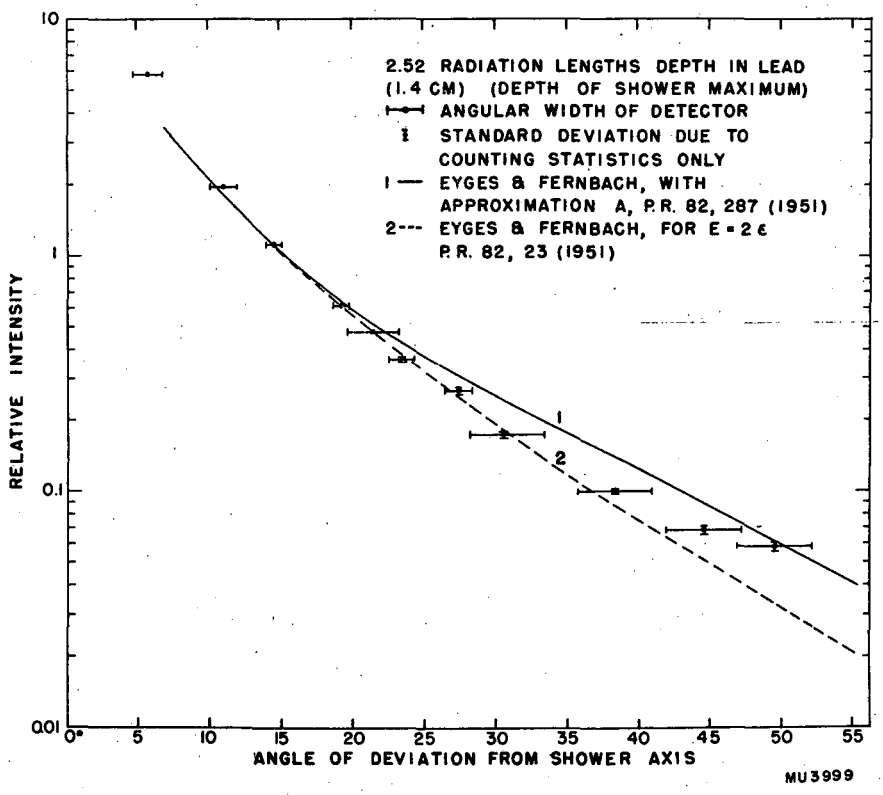
2.52 RADIATION LENGTHS DEPTH IN LEAD
(1.4 CM) (DEPTH OF SHOWER MAXIMUM)
ANGULAR WIDTH OF DETECTOR
STANDARD DEVIATION DUE TO
COUNTING STATISTICS ONLY
1 — EYGES & FERNBACH, WITH
APPROXIMATION A, P.R. 82, 287 (1951)
2--- EYGES & FERNBACH, FOR E = 2 ε
P.R. 82, 23 (1951)
RELATIVE INTENSITY
10
1
0.1
0.01
0°
5
10
15
20
25
30
35
40
45
50
55
ANGLE OF DEVIATION FROM SHOWER AXIS
MU3999

Fig. 4

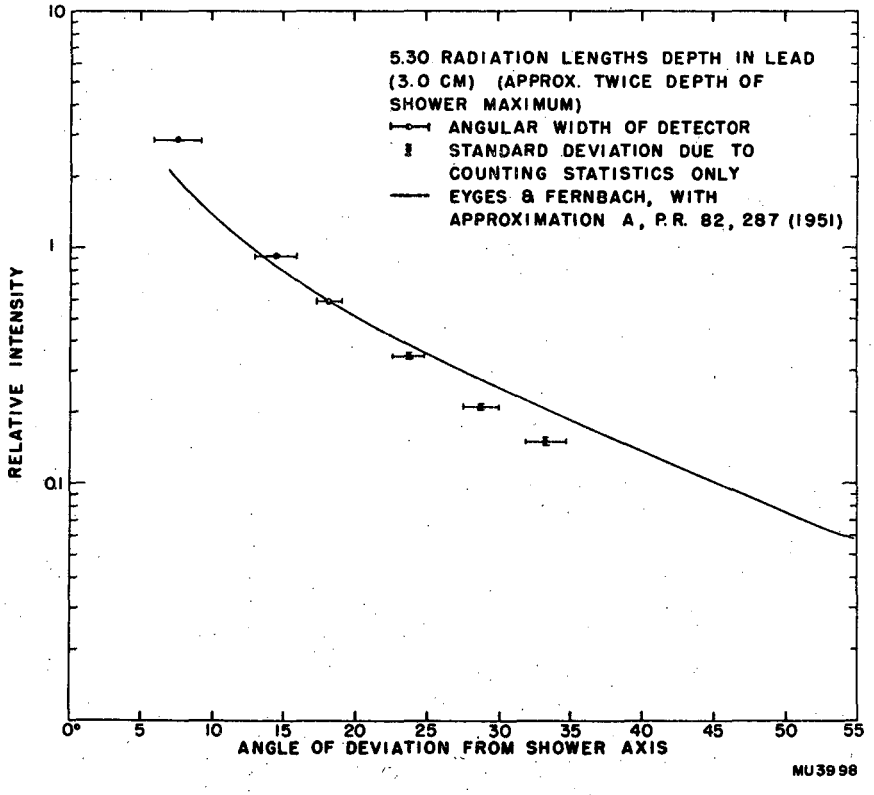
5.30 RADIATION LENGTHS DEPTH IN LEAD (3.0 CM) (APPROX. TWICE DEPTH OF SHOWER MAXIMUM)
ANGULAR WIDTH OF DETECTOR
STANDARD DEVIATION DUE TO COUNTING STATISTICS ONLY
EYGES & FERNBACH, WITH APPROXIMATION A, P.R. 82, 287 (1951)
RELATIVE INTENSITY
10
1
0.1
0°
5
10
15
20
25
30
35
40
45
50
55
ANGLE OF DEVIATION FROM SHOWER AXIS
MU3998

Fig. 5

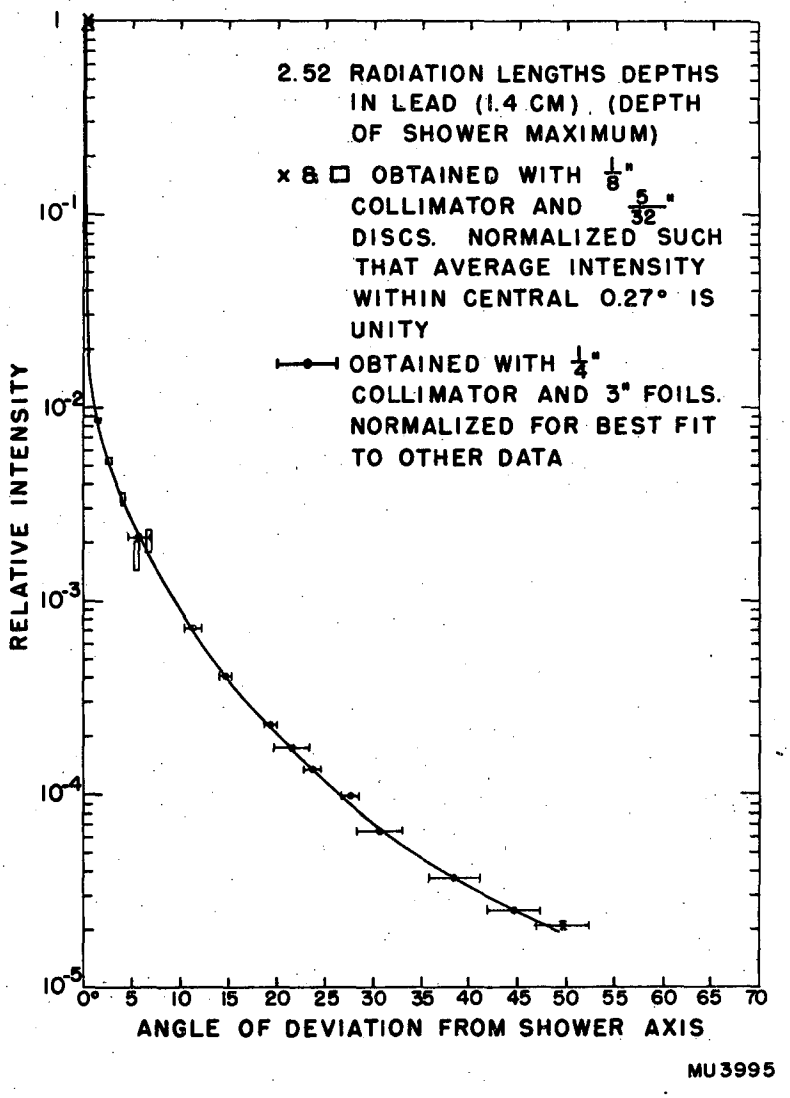
2.52 RADIATION LENGTHS DEPTHS IN LEAD (1.4 CM). (DEPTH OF SHOWER MAXIMUM)
× & □ OBTAINED WITH 1/8" COLLIMATOR AND 5/32" DISCS. NORMALIZED SUCH THAT AVERAGE INTENSITY WITHIN CENTRAL 0.27° IS UNITY
OBTAINED WITH 1/4" COLLIMATOR AND 3" FOILS. NORMALIZED FOR BEST FIT TO OTHER DATA
RELATIVE INTENSITY
1
10⁻¹
10⁻²
10⁻³
10⁻⁴
10⁻⁵
0° 5 10 15 20 25 30 35 40 45 50 55 60 65 70
ANGLE OF DEVIATION FROM SHOWER AXIS
MU3995

Fig. 6

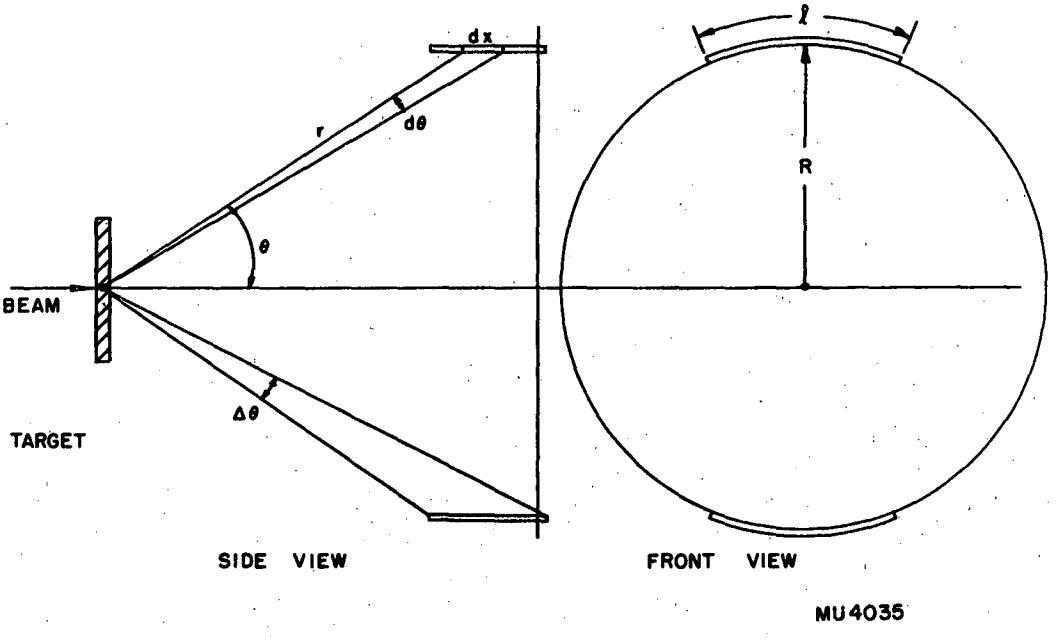

Fig. 7

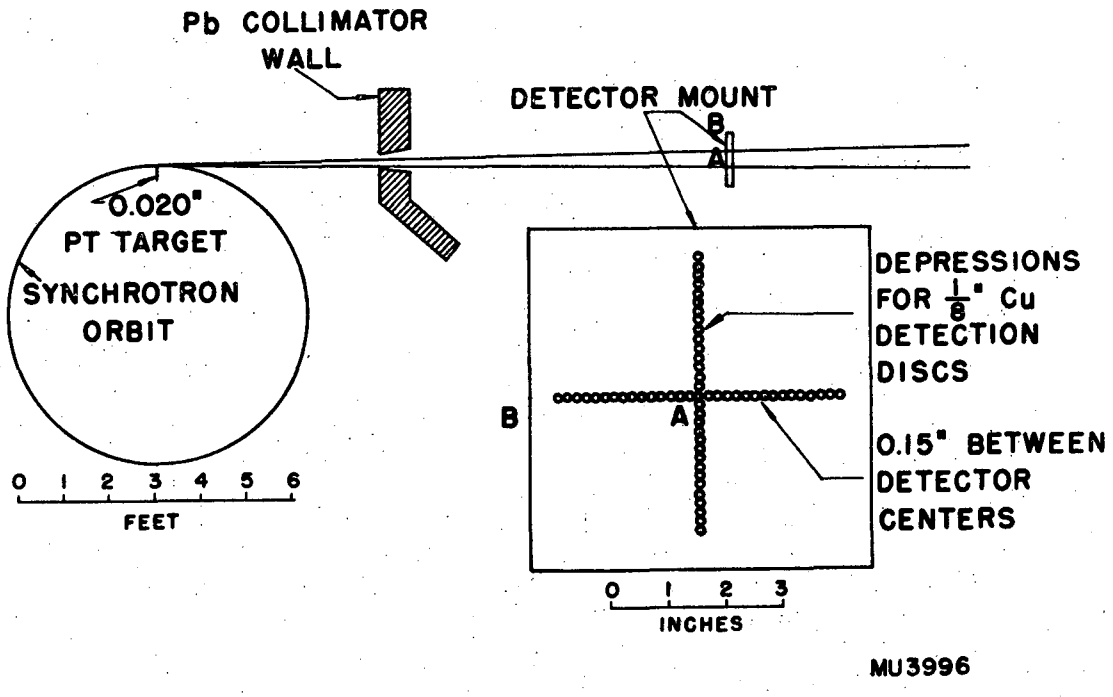
Pb COLLIMATOR WALL
DETECTOR MOUNT
B
A
0.020"
PT TARGET
SYNCHROTRON ORBIT
0 1 2 3 4 5 6
FEET
DEPRESSIONS FOR 1/8" Cu DETECTION DISCS
0.15" BETWEEN DETECTOR CENTERS
B
A
0 1 2 3
INCHES
MU3996

Fig. 8

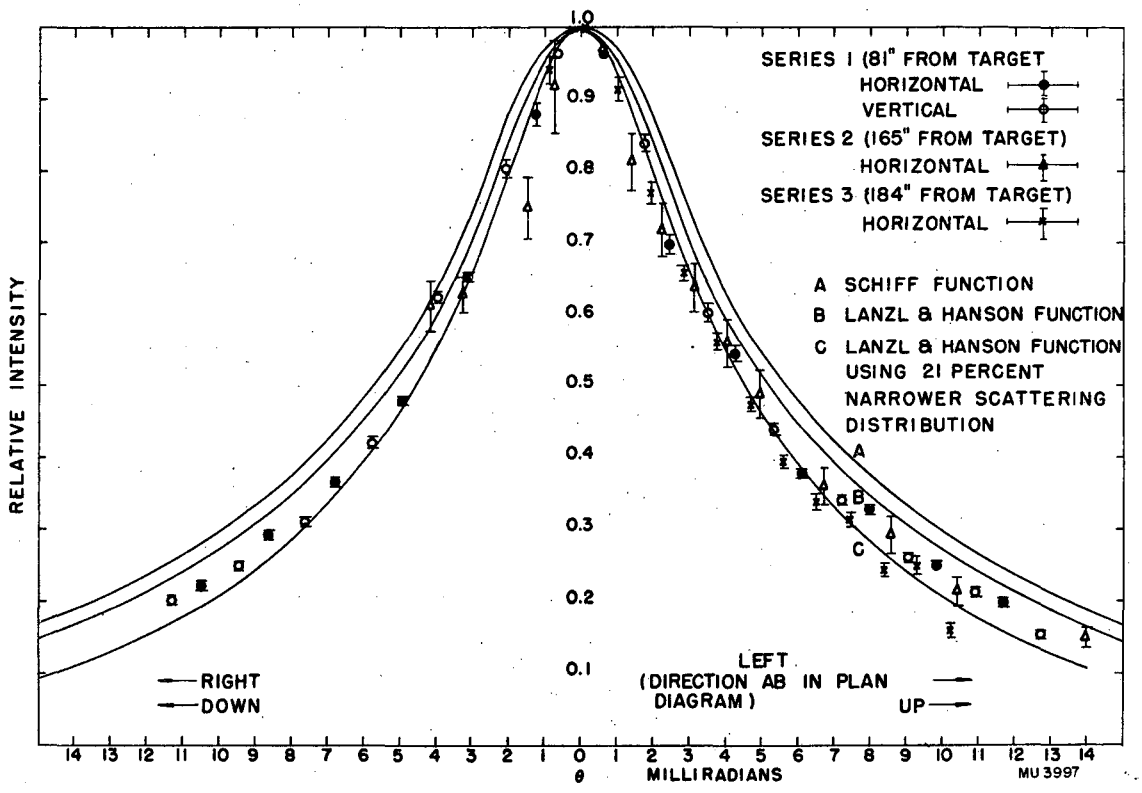
RELATIVE INTENSITY
1.0
0.9
0.8
0.7
0.6
0.5
0.4
0.3
0.2
0.1
SERIES 1 (81" FROM TARGET
HORIZONTAL
VERTICAL
SERIES 2 (165" FROM TARGET)
HORIZONTAL
SERIES 3 (184" FROM TARGET)
HORIZONTAL
A SCHIFF FUNCTION
B LANZL & HANSON FUNCTION
C LANZL & HANSON FUNCTION USING 21 PERCENT NARROWER SCATTERING DISTRIBUTION
A
B
C
RIGHT
DOWN
LEFT
(DIRECTION AB IN PLAN DIAGRAM)
UP
14 13 12 11 10 9 8 7 6 5 4 3 2 1 0 1 2 3 4 5 6 7 8 9 10 11 12 13 14
θ
MILLIRADIANS
MU 3997

Fig. 9

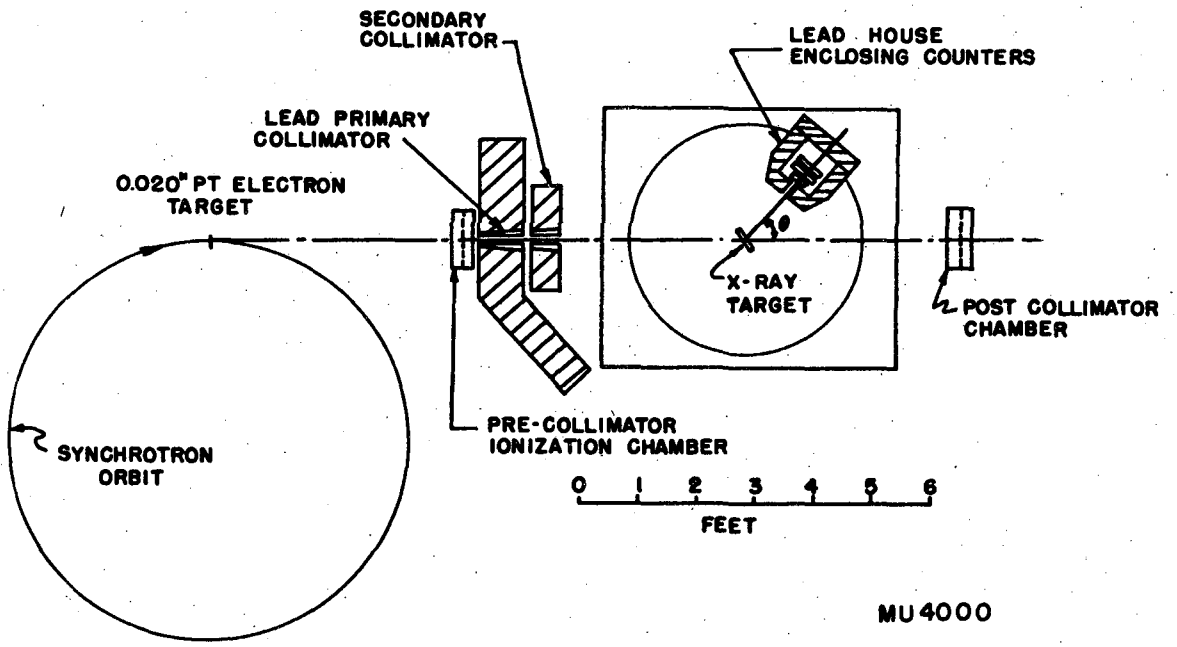
SECONDARY COLLIMATOR
LEAD HOUSE ENCLOSING COUNTERS
LEAD PRIMARY COLLIMATOR
0.020" PT ELECTRON TARGET
θ
X-RAY TARGET
POST COLLIMATOR CHAMBER
SYNCHROTRON ORBIT
PRE-COLLIMATOR IONIZATION CHAMBER
0 1 2 3 4 5 6
FEET
MU4000

Fig. 10

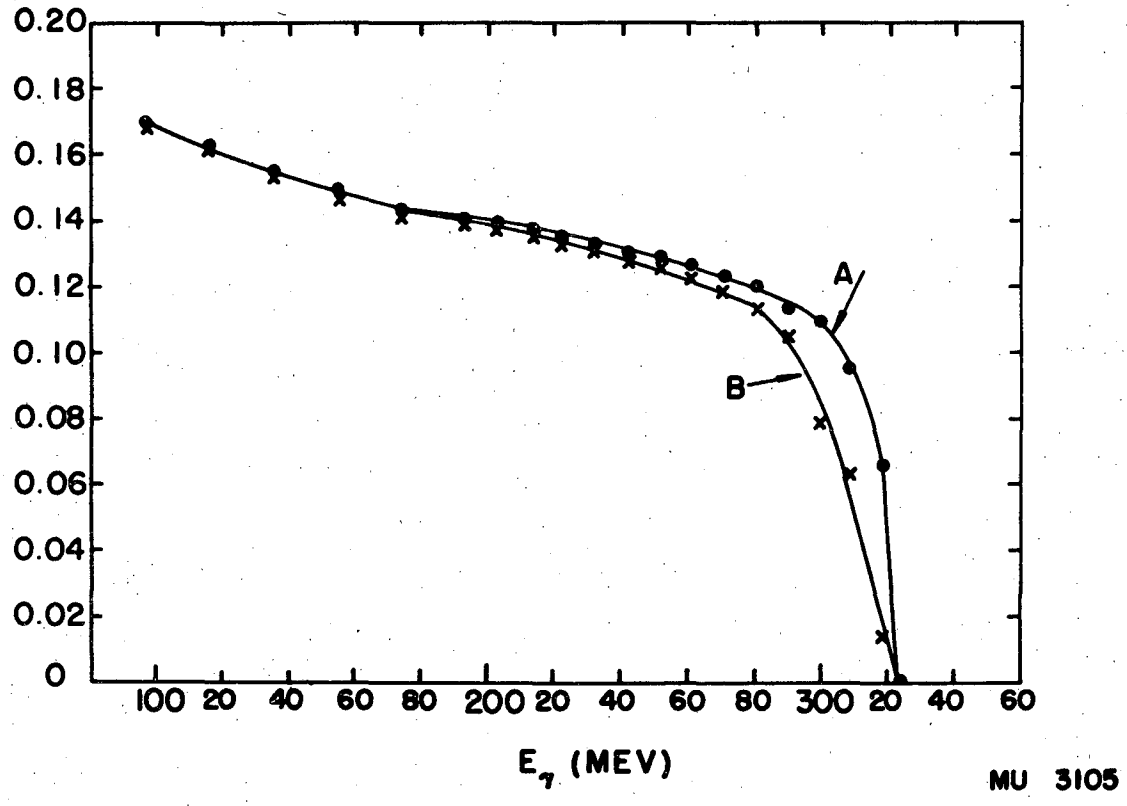
0.20
0.18
0.16
0.14
0.12
0.10
0.08
0.06
0.04
0.02
0
100 20 40 60 80 200 20 40 60 80 300 20 40 60
A
B
E_γ (MEV)
MU 3105

Fig. 11

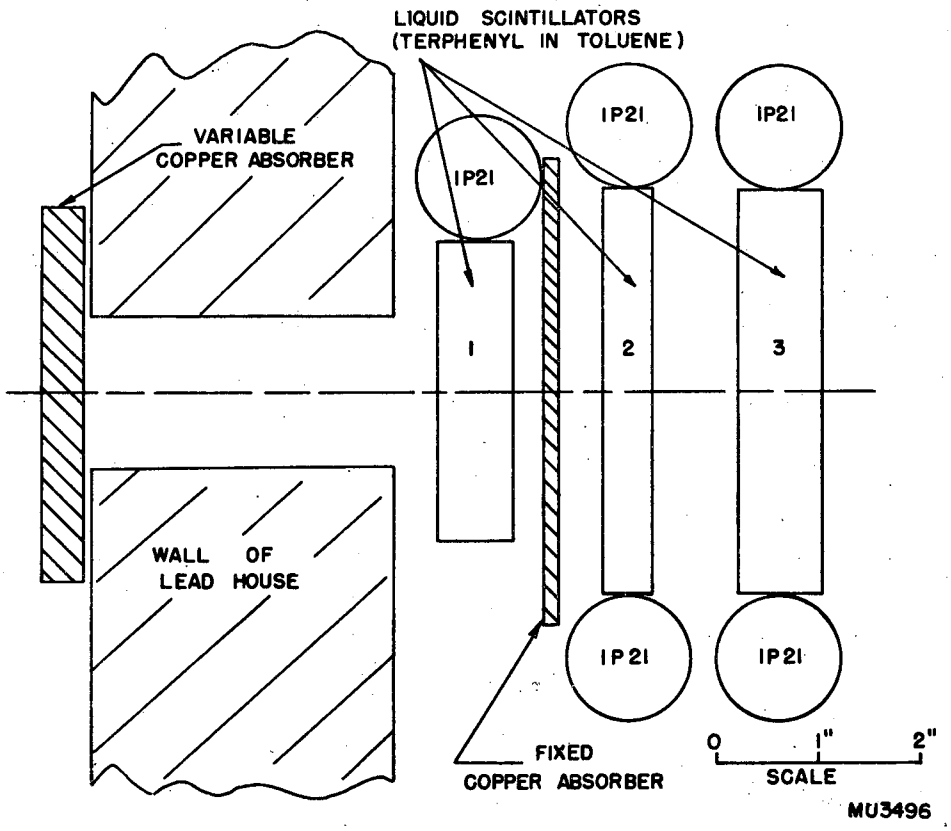
LIQUID SCINTILLATORS
(TERPHENYL IN TOLUENE)
VARIABLE
COPPER ABSORBER
IP21
IP21
IP21
1
2
3
WALL OF
LEAD HOUSE
IP21
IP21
FIXED
COPPER ABSORBER
0
1"
2"
SCALE
MU3496

Fig. 12

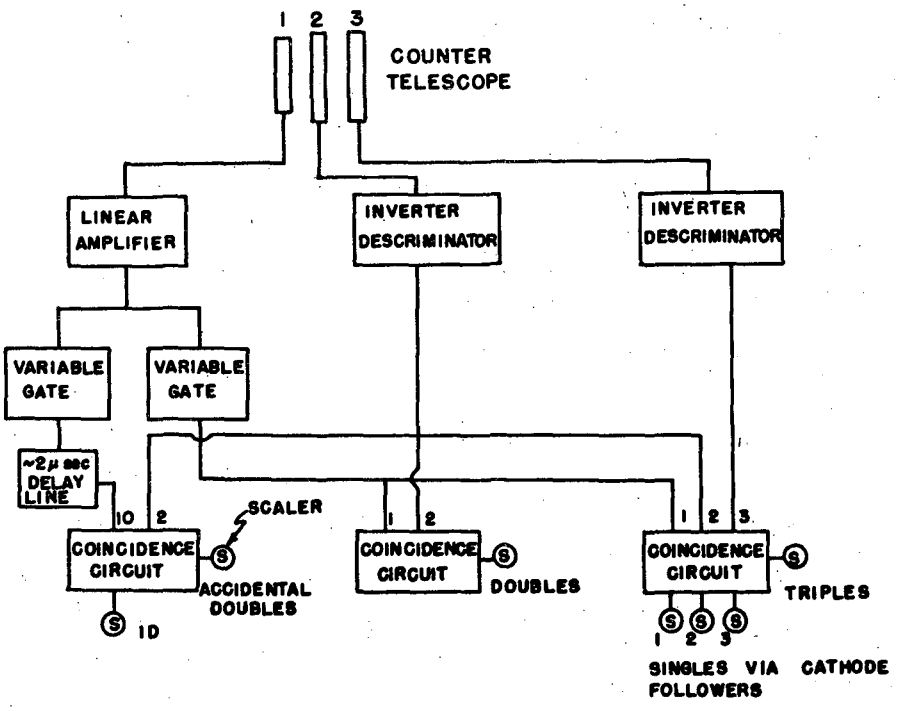
1 2 3
COUNTER TELESCOPE
LINEAR AMPLIFIER
INVERTER DESCRIMINATOR
INVERTER DESCRIMINATOR
VARIABLE GATE
VARIABLE GATE
~2μ sec DELAY LINE
10 2
SCALER
COINCIDENCE CIRCUIT
ACCIDENTAL DOUBLES
1D
1 2
COINCIDENCE CIRCUIT
DOUBLES
1 2 3
COINCIDENCE CIRCUIT
TRIPLES
1 2 3
SINGLES VIA CATHODE FOLLOWERS
MU 4002

Fig. 13

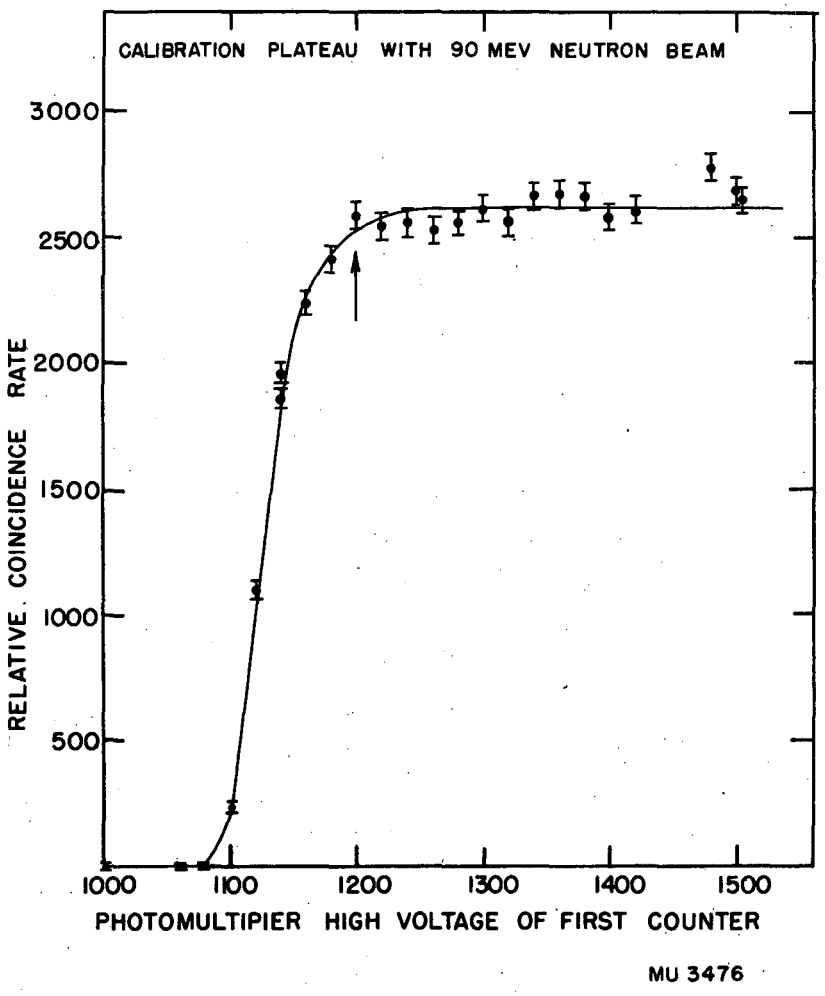
CALIBRATION PLATEAU WITH 90 MEV NEUTRON BEAM
RELATIVE COINCIDENCE RATE
3000
2500
2000
1500
1000
500
1000
1100
1200
1300
1400
1500
PHOTOMULTIPIER HIGH VOLTAGE OF FIRST COUNTER
MU 3476

Fig. 14

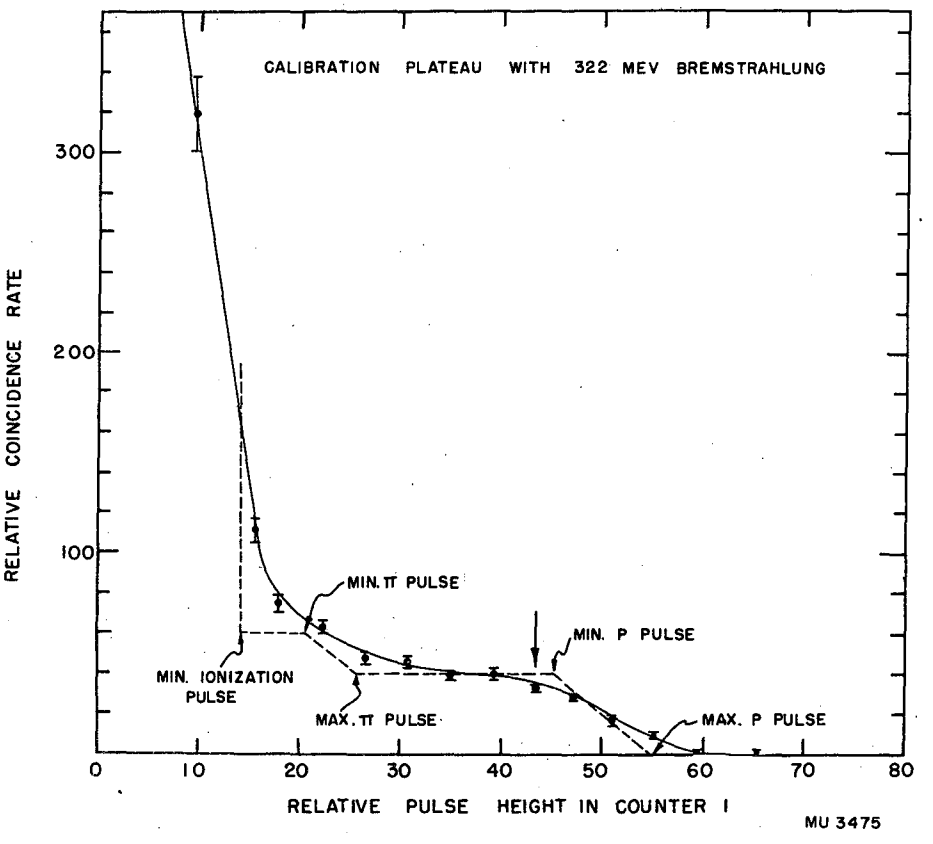
CALIBRATION PLATEAU WITH 322 MEV BREMSTRAHLUNG
RELATIVE COINCIDENCE RATE
300
200
100
0
10
20
30
40
50
60
70
80
RELATIVE PULSE HEIGHT IN COUNTER I
MIN. IONIZATION PULSE
MIN. π PULSE
MAX. π PULSE
MIN. P PULSE
MAX. P PULSE
MU 3475

Fig. 15

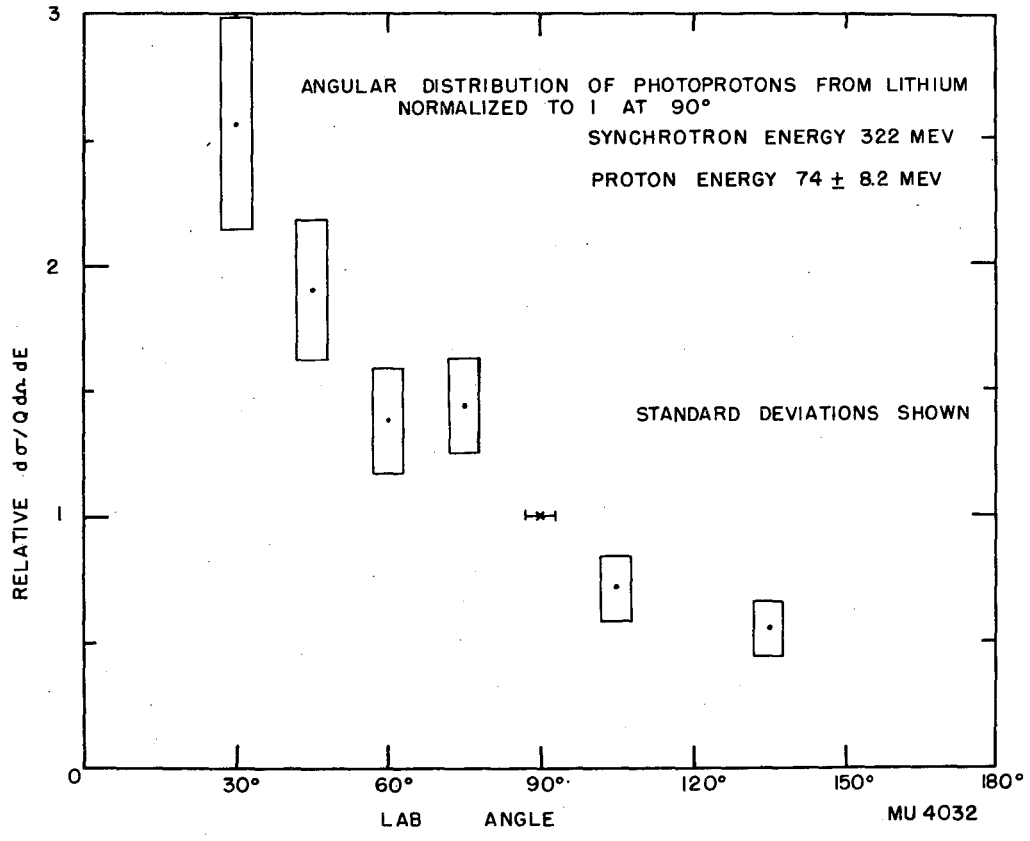
ANGULAR DISTRIBUTION OF PHOTOPROTONS FROM LITHIUM
NORMALIZED TO 1 AT 90°
SYNCHROTRON ENERGY 322 MEV
PROTON ENERGY 74 ± 8.2 MEV
STANDARD DEVIATIONS SHOWN
RELATIVE dσ/Ωdn. dE
3
2
1
0
30°
60°
90°
120°
150°
180°
LAB ANGLE
MU 4032

Fig. 16

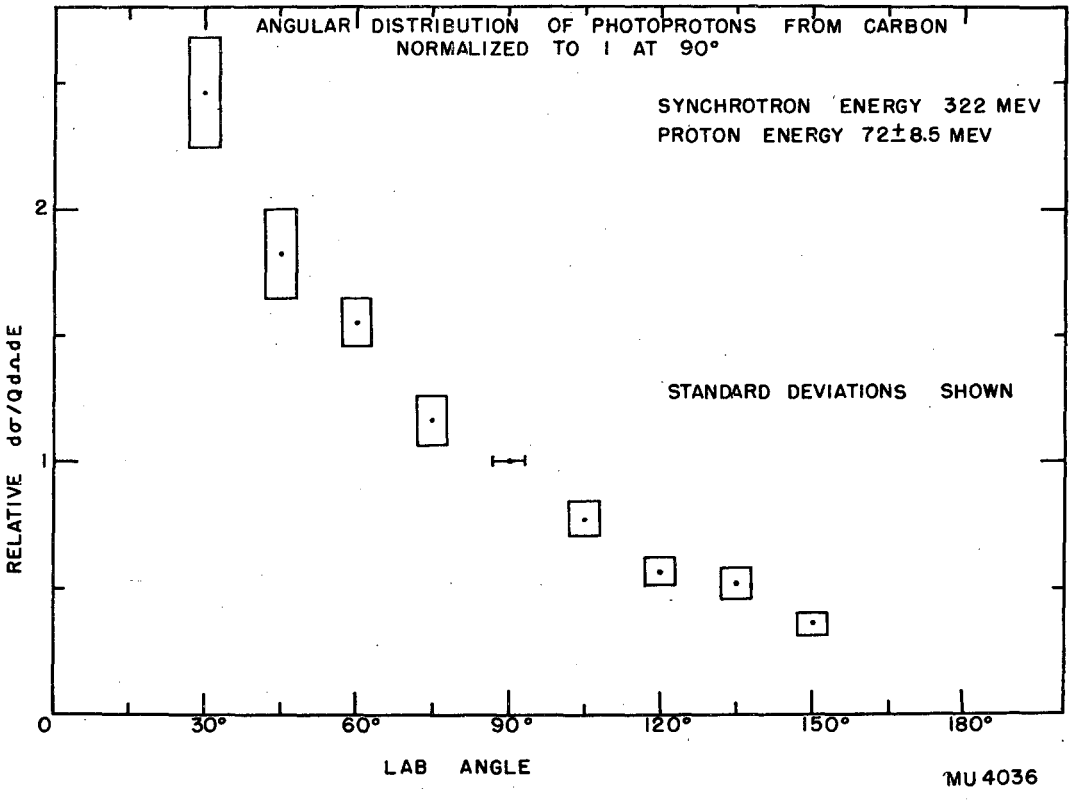
ANGULAR DISTRIBUTION OF PHOTOPROTONS FROM CARBON
NORMALIZED TO 1 AT 90°
SYNCHROTRON ENERGY 322 MEV
PROTON ENERGY 72±8.5 MEV
STANDARD DEVIATIONS SHOWN
RELATIVE dσ/Ωdn.dE
0
1
2
30°
60°
90°
120°
150°
180°
LAB ANGLE
MU 4036

Fig. 17

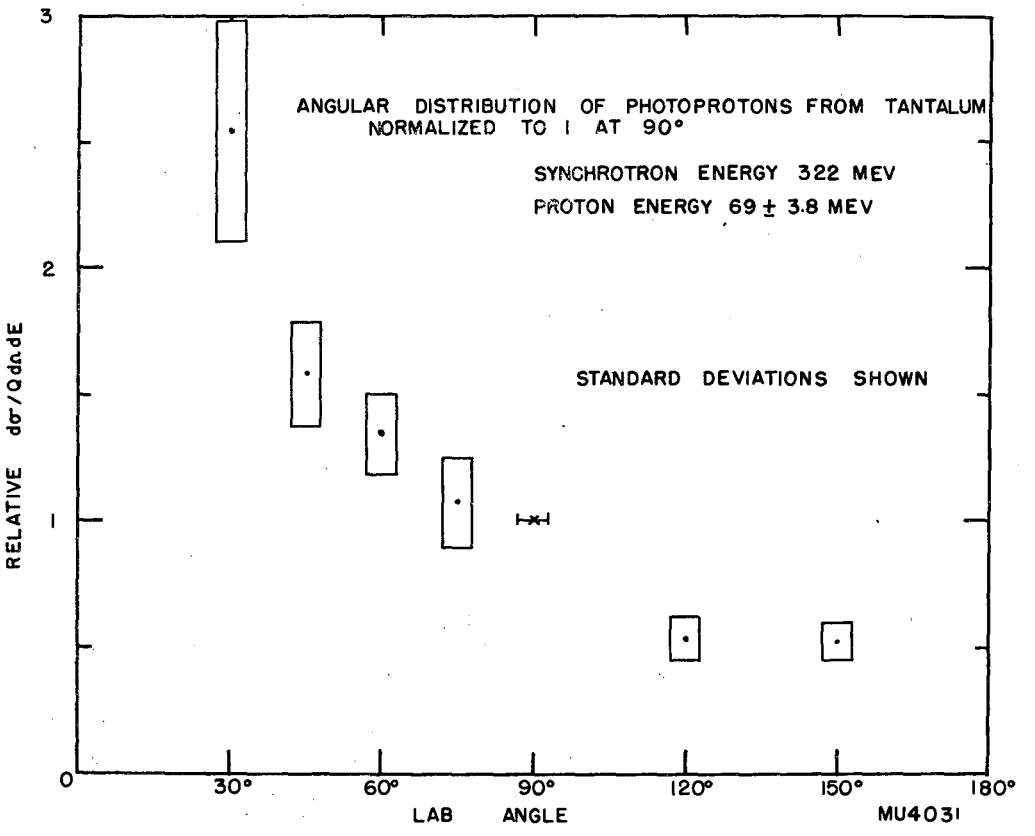
ANGULAR DISTRIBUTION OF PHOTOPROTONS FROM TANTALUM
NORMALIZED TO 1 AT 90°
SYNCHROTRON ENERGY 322 MEV
PROTON ENERGY 69 ± 3.8 MEV
STANDARD DEVIATIONS SHOWN
RELATIVE dσ/Ωdα.dE
3
2
1
0
30°
60°
90°
120°
150°
180°
LAB ANGLE
MU4031

Fig. 18

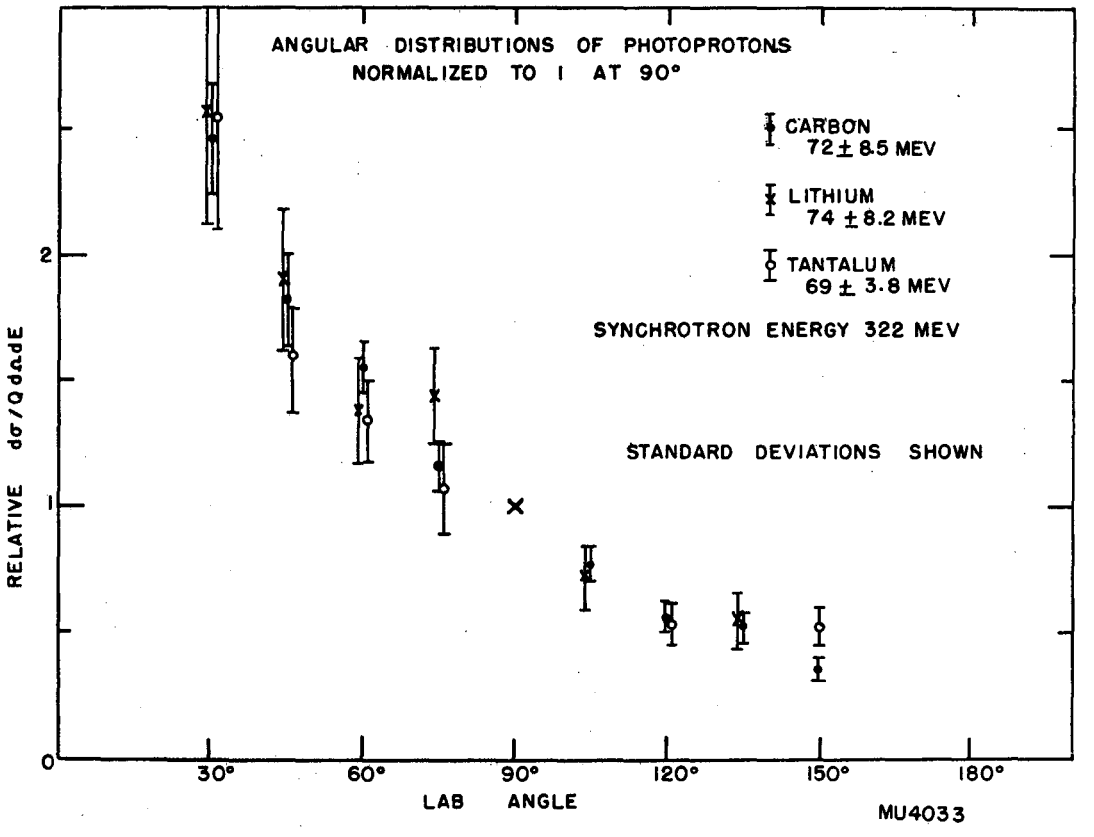
ANGULAR DISTRIBUTIONS OF PHOTOPROTONS
NORMALIZED TO 1 AT 90°
CARBON
72 ± 8.5 MEV
LITHIUM
74 ± 8.2 MEV
TANTALUM
69 ± 3.8 MEV
SYNCHROTRON ENERGY 322 MEV
STANDARD DEVIATIONS SHOWN
RELATIVE dσ/Qdadε
0
1
2
30°
60°
90°
120°
150°
180°
LAB ANGLE
MU4033

Fig. 19

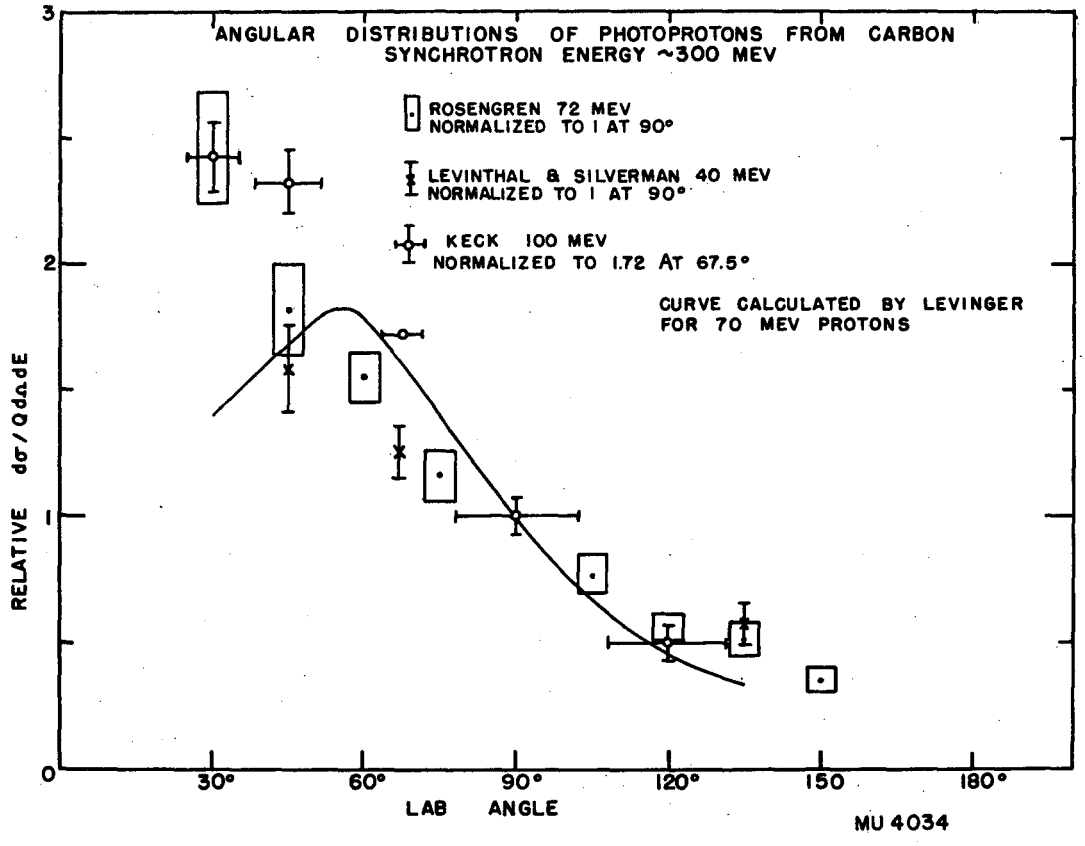
ANGULAR DISTRIBUTIONS OF PHOTOPROTONS FROM CARBON
SYNCHROTRON ENERGY ~300 MEV
ROSENGREN 72 MEV
NORMALIZED TO I AT 90°
LEVINTHAL & SILVERMAN 40 MEV
NORMALIZED TO I AT 90°
KECK 100 MEV
NORMALIZED TO 1.72 AT 67.5°
CURVE CALCULATED BY LEVINGER
FOR 70 MEV PROTONS
RELATIVE dσ/QdΩdE
3
2
1
0
30°
60°
90°
120°
150
180°
LAB ANGLE
MU 4034

Fig. 20

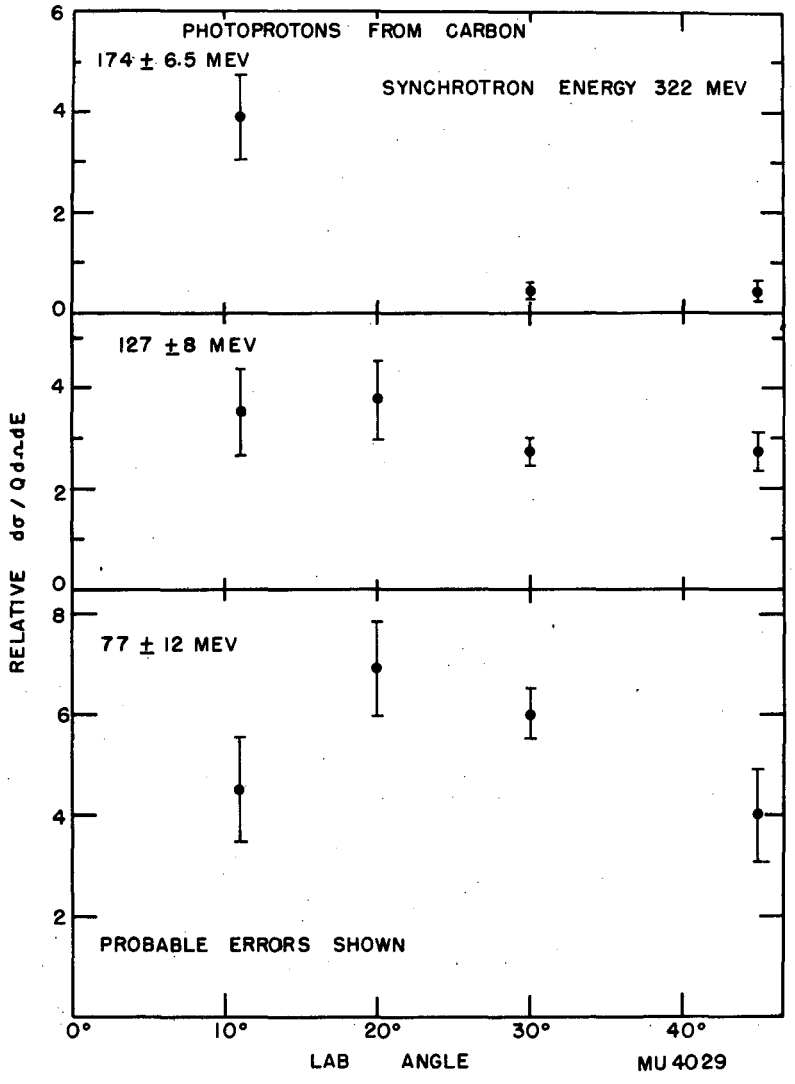
PHOTOPROTONS FROM CARBON
174 ± 6.5 MEV
SYNCHROTRON ENERGY 322 MEV
127 ±8 MEV
77 ± 12 MEV
PROBABLE ERRORS SHOWN
RELATIVE dσ / Qdωdε
0°
10°
20°
30°
40°
LAB ANGLE
MU 4029

Fig. 21

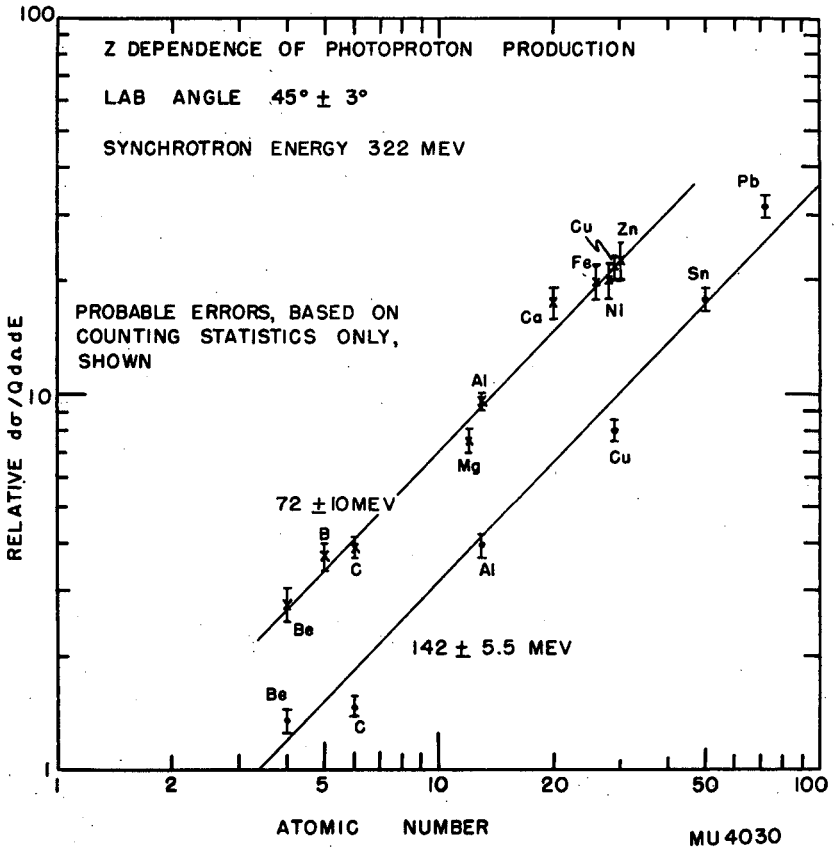
Z DEPENDENCE OF PHOTOPROTON PRODUCTION
LAB ANGLE 45° ± 3°
SYNCHROTRON ENERGY 322 MEV
PROBABLE ERRORS, BASED ON COUNTING STATISTICS ONLY, SHOWN
72 ± 10 MEV
142 ± 5.5 MEV
RELATIVE dσ/dΩdE
ATOMIC NUMBER
MU4030
100
10
1
1
2
5
10
20
50
100
Be
B
C
Al
Mg
Ca
Fe
Cu
Zn
Ni
Sn
Pb

Fig. 22

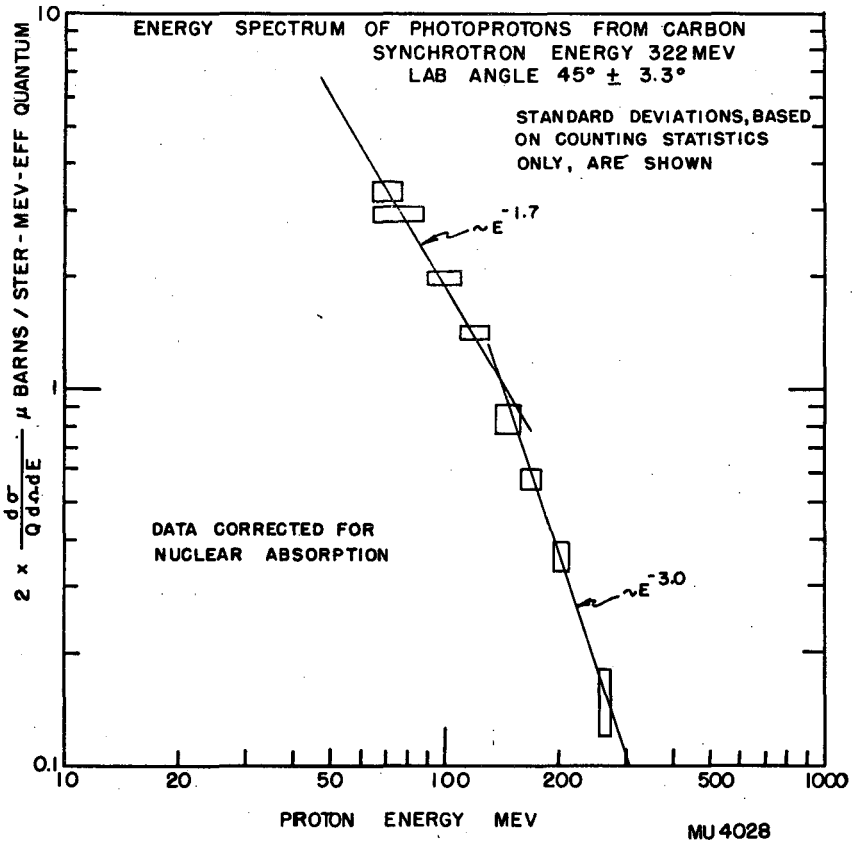
ENERGY SPECTRUM OF PHOTOPROTONS FROM CARBON
SYNCHROTRON ENERGY 322 MEV
LAB ANGLE 45° ± 3.3°
STANDARD DEVIATIONS, BASED ON COUNTING STATISTICS ONLY, ARE SHOWN
~E^-1.7
~E^-3.0
DATA CORRECTED FOR NUCLEAR ABSORPTION
2 x dσ/Qdωd E · μ BARNS / STER - MEV - EFF QUANTUM
10
1
0.1
10
20
50
100
200
500
1000
PROTON ENERGY MEV
MU 4028

Fig. 23

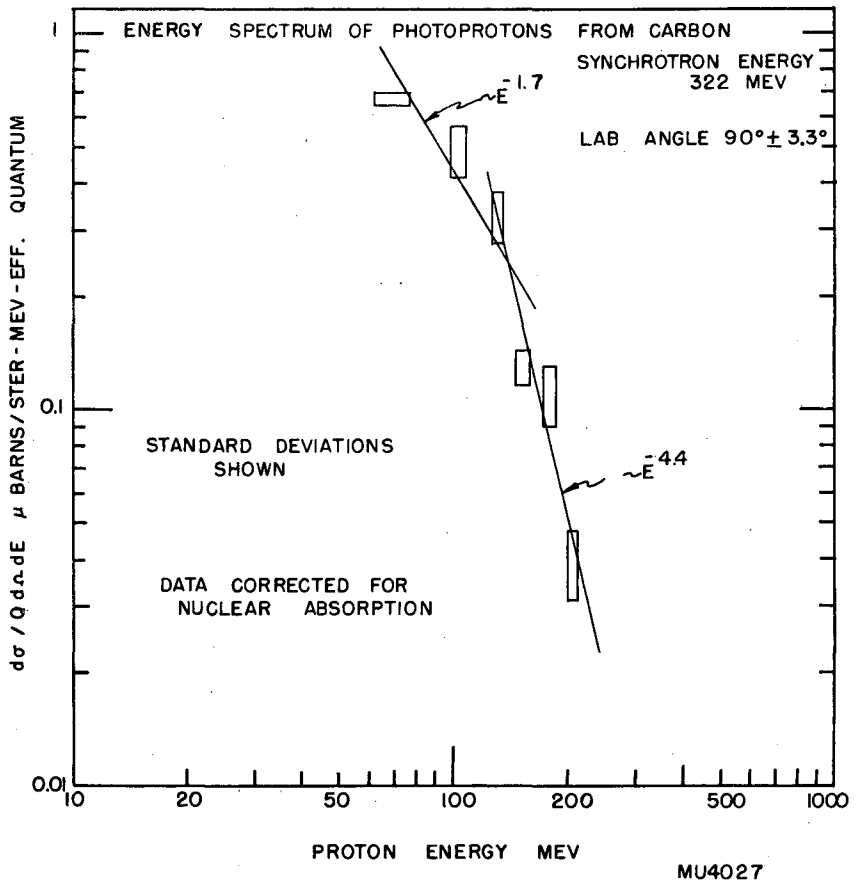
ENERGY SPECTRUM OF PHOTOPROTONS FROM CARBON
SYNCHROTRON ENERGY
322 MEV
LAB ANGLE 90° ± 3.3°
~E^-1.7
~E^-4.4
STANDARD DEVIATIONS
SHOWN
DATA CORRECTED FOR
NUCLEAR ABSORPTION
dσ / Q dΩ dE μ BARNS/STER-MEV-EFF. QUANTUM
1
0.1
0.01
10
20
50
100
200
500
1000
PROTON ENERGY MEV
MU4027

Fig. 24